An Active Disturbance Rejection Controlled Quadrotor Slung-Load System for use in Water Sampling Excursions

Έλεγχος με μεθοδολογία Active Disturbance Rejection Control ενός UAV τεσσάρων ελίκων με αναρτημένο δοχείο για δειγματοληψεία υδάτινων περιοχών.

Alexopoulos Aggelos

Supervising Professor: Konstantinos Kyriakopoulos

A THESIS SUBMITTED IN PARTIAL FULFILMENT OF THE REQUIREMENTS FOR THE DEGREE OF

MASTER OF SCIENCE
in
"Automation Systems" National Technical University of Athens

Athens, Greece
Semptember 2021

ABSTRACT

The subject of this thesis is the modelling and control of a quadrotor slung-load system. The purpose of this system is to gather samples from bodies of water. A small cannister is slung by a cable onto the quadrotor's frame. Then, the quadrotor flies over the point of interest and immerses the cannister in the water. When it fills up, the quadrotor returns to its take-off point to bring the sample back. While the cannister is in the water, it is subjected to forces from various currents. These forces can draw the quadrotor away from the initial point of interest. A control law based on the Active Disturbance Rejection Control methodology will be developed, to mitigate the influence of the current disturbances on the system. The performance of this controller will be compared to the normal PID and the advantages and disadvantages of each controller will be evaluated.

CONTENTS

ACKNOWLEDGEMENTS

Through the taxing but rewarding process of working on this thesis, the author found support in numerous people. Firstly, the valuable feedback of Professor K.Kyriakopoulos and post-doctoral researcher Ch.Bechlioulis must be acknowledged , and especially the monthly progress meeting, which kept the author alert and involved with the work. Secondly, the support of his friends who provided a release in the form of a walk in the park or at the city square for a quick beverage. And, finally the presence of his family, who have patiently supported him in all his endeavours through the years.

Thanks are also due to the people that helped the author pursue studies in this MSc program. To Professor D. Reissis of Athens Kapodistrian University's Physics Department for recommending the subject of the author's bachelor thesis, essentially ushering him in the world of engineering. And to Professor K.Tzafestas for his encouragement to apply to this MSc program.

Finally, an offer of kind thanks is due to the author's costudents D.Albani and J.Balatsoukas for the wonderful times of putting together a quadrotor and having the joy and agony of watching it fly then crash, many many times.

INTRODUCTION

A quadrotor belongs to the family of multirotor Unmaned Aerial Vehicles. By strapping multiple motors symmetrically on a frame and by equipping these motors with propellers, we can have a flying platform. But the system is not a hundred per cent symmetrical like anything in the real world cannot ever be the exact copy of something else. There might be minor differences in the motors, or the propellers, or small differentiations in the moments of inertia of its principal axes. So, an open loop system with diametrically opposed spinning propellers will never truly fly stably. Even if they were exactly the same a gust of wind would immediately destabilise it. There must be a way to ensure balance. With developments in material technologies, computers and electronic sensors begun to shrink. Their installation became possible on small vehicle frames. This is where the multirotor UAV was born. The basic idea is that by sensing the frame's angle with a gyroscopic sensor the onboard computer can calculate the frame's derivation from its wanted attitude and through a control algorithm (most frequently proportional-integral-derivative or PID) send signals to the motors to correct the attitude and bring balance to the vehicle. A simple but powerful idea that enables these machines to fly with immaculate precision.

Precision is the key word, explaining the popularity of multirotors. Helicopter and multirotor advantages over fixed wing aircraft is their ability of Vertical Take Off and Landing (VTOL), as well as the ability to occupy an airborne position with zero spatial velocity. In contrast, a fixed wing aircraft has to move in order to generate lift and keep flying. Thus, multirotors and helicopters are ideal for tasks requiring precise manoeuvring such as photography, acrobatic movements, picking or dropping payloads, and more. When compared to helicopters, multirotors come out on top in terms of precision. Their structure is "more" symmetrical, granting them additional agility. When a multirotor needs to move towards a direction it simply tilts towards that direction, in contrast to a helicopter which first needs to turn, face the direction, and then tilt towards it. The reason multirotors have not replaced helicopters heavier than 25 kilograms is that, at those weights, one big internal combustion motor is much more efficient than many electrical motors, or many smaller internal combustion motors. Currently multirotors are dominating the market of small UAVs and find diverse applications across multiple projects. Among its many uses, the multirotor can also be used for water sampling. Its agility, ease of deployment and small size allow it to sample from water bodies that are difficult to reach, relieve the person from gathering the sample himself/herself and, in any case, facilitate the whole process.

The contribution of this thesis regarding this water sampling application is the following:

Chapter 1 describes the modelling of a simple quadrotor starting from basic Lagrangian mechanics, then explains using the Intermediate Axis Theorem that it is inher-

ently unstable, and finally describes the cascade PID controller that stabilises it.

Chapter 2 deals thoroughly with the modelling of the quadrotor slung-load system.

Chapter 3 gives examples of the methodology behind the ADRC, then describes the control scheme to be used for the slung-load system, a PD-ADRC cascade controller that is system agnostic and simple to tune.

Chapter 4 analyses the results of simulations using both the PID and the PD-ADRC, while subjecting the slung-load system to various disturbances from wind gusts, and water currents. The results are compared and conclusions are extracted. All simulations are done in the Matlab/Simulink environment.

Chapter 5, the Appendix, contains various proofs and concepts that while necessary to understand the subject of the thesis, their inclusion in the main text would be disruptive to the flow of explanation going on in each chapter. Thus to have more clear reasoning in each chapter, some information was moved in the Appendix.

1. DYNAMIC MODEL AND CONTROL OF A QUADROTOR UAV

This section is devoted to a quadrotor's general working principles, it's mechanical modelling and the control schemes that enable it to fly. At this point, we proceed to analyse how the dynamic model of a quadrotor is derived and, subsequently, how it is controlled with a cascade PID structure. This analysis will put to scope the changes we'll perform on both the model and the control scheme, when we change over to a slung-load system controlled by a PD-ADRC controller.

We define two inertial coordinate systems, one fixed on the earth called the earth inertial frame, and one fixed on the body, always having the same orientation as the body, called the body-fixed frame. The following figure exhibits these two frames:

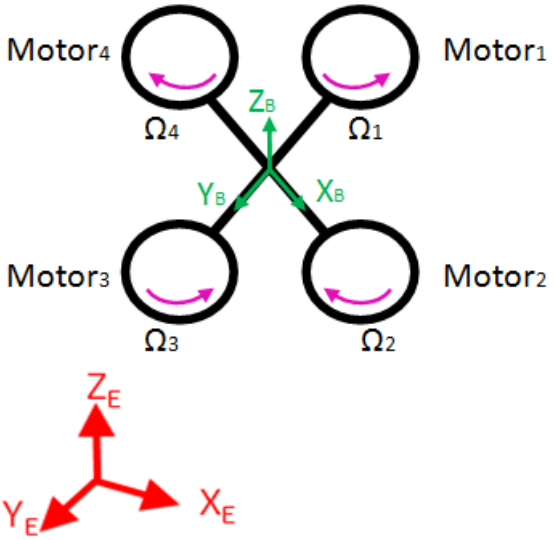

Fig. 1.1: Earth Frame(red) and Body-Fixed Frame(green)

.

Why define two coordinate systems instead of just the earth inertial frame?
Because we can take the best of both worlds. The earth frame is best for expressing the translational movement of the vehicle, while the body-fixed frame is best for expressing the rotational movement.
Why so?
Being stranded on the vehicle, always with the same orientation(as shown in Figure 1) the body-fixed frame always sees the same moment of inertia for the quadrotor, in contrast with the earth frame which, as the quadrotor rotates, sees the moment of inertia vary as time goes on. Therefore it is much simpler to calculate angular accelerations on the body fixed frame. In subsection 5.1 of the Appendix, a brief review of Euler angles, Rotation

Matrices and Matrix T_Θ can be found. Moving forward, it is taken as granted that those concepts are well known.

It is possible to pick a hybrid vector of coordinates, with which to describe translational and angular velocity for the quadrotor. Define vector ξ as:

$$\xi = \begin{bmatrix} \mathrm{X} \\ \Upsilon \\ \mathrm{Z} \\ \phi \\ \theta \\ \psi \end{bmatrix}$$

where X,Y,Z are the coordinates of the vehicle's Center of Mass (abbreviated as CM) and ϕ, θ, ψ are the Euler angles of the vehicle's current attitude. Vector ξ gives a full picture of the quadrotor's posture and position in space. The vector of the quadrotor's velocities in the body-frame will be:

$$v = \begin{bmatrix} u \\ v \\ w \\ p \\ q \\ r \end{bmatrix}$$

The two are connected with the following equation:

$$\dot{\xi} = \begin{bmatrix} R_\Theta & 0 \\ 0 & \mathrm{T}_\Theta \end{bmatrix} u$$

As we've seen earlier, in order to describe the dynamics of the quadrotor it is preferable to analyse the rotational dynamics in the body-fixed frame instead of the earth inertial frame. Thus, we denote a hybrid system H, one that combines the translational velocities of the earth frame with the rotational velocities of the body-fixed frame. The velocities in this hybrid system are neatly contained in vector ζ:

$$\zeta = \begin{bmatrix} \dot{\mathrm{X}} \\ \dot{\Upsilon} \\ \dot{\mathrm{Z}} \\ p \\ q \\ r \end{bmatrix}$$

The first three elements of the vector are the spatial velocities expressed in E-frame, while the last three elements are the rotational velocities in B-frame. Now on to derive the dynamics of the vehicle. According to Mechanics, the Lagrangian of a rigid body is the sum of the translational kinetic energy of its center mass plus its rotational kinetic energy. Translational kinetic energy of CM would be:

$$\frac{1}{2}\begin{bmatrix} \dot{X} \\ \dot{Y} \\ \dot{Z} \end{bmatrix}^T \begin{bmatrix} M_q & 0 & 0 \\ 0 & M_q & 0 \\ 0 & 0 & M_q \end{bmatrix} \begin{bmatrix} \dot{X} \\ \dot{Y} \\ \dot{Z} \end{bmatrix} = \frac{1}{2} {u_E}^T \begin{bmatrix} M_q & 0 & 0 \\ 0 & M_q & 0 \\ 0 & 0 & M_q \end{bmatrix} u_E$$

while rotational K.E. would be, in the earth inertial frame :

$$\frac{1}{2}{\omega_E}^T I_E \omega_E$$

where ω_E denotes the vehicle's angular velocity in E-frame and I_E is the moment of inertia matrix in the same frame. Therefore Kinetic Energy total is:

$$KE = L = KE_{q,tr,E} + KE_{q,rot,E} \tag{1.1}$$

It's high time to apply the Euler-Lagrange equations to the current Lagrangian to find the quadrotor's dynamics:

$$\frac{d}{dt}\begin{bmatrix} \frac{d}{du_E} \\ \frac{d}{d\omega_E} \end{bmatrix} L + \begin{bmatrix} \frac{d}{dx_E} \\ \frac{d}{d\theta_E} \end{bmatrix} L = \begin{bmatrix} F_E \\ P_E \end{bmatrix}$$

where $u_E = \begin{bmatrix} \dot{X} & \dot{Y} & \dot{Z} \end{bmatrix}^T$ is the vector of translational velocity, $\omega_E = \begin{bmatrix} \omega_x & \omega_y & \omega_z \end{bmatrix}^T$ is the vector of rotational velocity, $x_E = \begin{bmatrix} X & Y & Z \end{bmatrix}^T$ is the spatial coordinates vector, and $\theta_E = \begin{bmatrix} angle_x & angle_y & angle_z \end{bmatrix}^T$ are the angles around axis x,y,z , $F_E = \begin{bmatrix} F_x & F_y & F_z \end{bmatrix}^T$ are any outside forces (gravity,wind, propellers) acting on the quadrotor and $P_E = \begin{bmatrix} P_x & P_y & P_z \end{bmatrix}^T$ are any outside torques (propellers, gyroscopic effect,wind turbulence) acting on the quadrotor. All these vectors are expressed in the E-frame.

The translational part gives us simply:

$$M_q \begin{bmatrix} \ddot{X} \\ \ddot{Y} \\ \ddot{Z} \end{bmatrix} = F_E$$

while the rotational part will be:

$$\frac{d}{dt}\frac{d}{d\omega_E}L + \frac{d}{d\theta_E}L = P_E$$

Since L has no dependence on θ_E and since $\frac{d}{d\omega_E}L = I_E\omega_E$ we get:

$$\frac{d}{dt}(I_E\omega_E) = P_E \Rightarrow \frac{d}{dt}(H_E) = P_E \tag{1.2}$$

where $H_E = I_E\omega_E$ is the vehicle's angular momentum in E-frame. We'll move to B-frame. First the following equation needs to be mentioned:

$$\frac{dR_\Theta}{dt} = S(\omega_E)R_\Theta \tag{1.3}$$

, where $S(\omega_E)$ is the skew-symmetric matrix of ω_E. The skew symmetric matrix of a vector A has the following property when multiplied with vector B :

$$S(\mathrm{A})\mathrm{B} = \mathrm{A} \times \mathrm{B}$$

Now, it's mandatory to find the relationship between the moment of inertia tensor in the E-frame, I_E , and the moment of inertia tensor in the B-frame I_B. The rotating body's angular momentum expressions in the E-frame and B-frame are connected, as usual, by the rotation matrix R_Θ:

$$H_E = R_\Theta H_B \Rightarrow I_E \omega_E = R_\Theta I_B \omega_B$$

by using the property of rotation matrices, ${R_\Theta}^{-1} R_\Theta = 1$, we get:

$$I_E \omega_E = R_\Theta I_B ({R_\Theta}^{-1} R_\Theta)\omega_B \Rightarrow I_E R_\Theta \omega_B = (R_\Theta I_B {R_\Theta}^{-1}) R_\Theta \omega_B \Rightarrow I_E = R_\Theta I_B {R_\Theta}^{-1} \quad (1.4)$$

A third equation that will be of use is:

$$\frac{d\mathrm{H}_B}{dt} = \mathrm{I}_B \dot{\omega}_B \quad (1.5)$$

which is true since I_B is a constant matrix.

Expanding on from relation (1.2) and using (1.3),(1.4),(1.5) we get:

$$\begin{aligned}
&\frac{d}{dt}(H_E) = P_E \Rightarrow \\
&\qquad \Rightarrow \frac{dR_\Theta}{dt}\mathrm{H}_B + R_\Theta \frac{d\mathrm{H}_B}{dt} = P_E \Rightarrow \\
&\qquad \Rightarrow S(\omega_E) R_\Theta \mathrm{H}_B + R_\Theta \mathrm{I}_B \dot{\omega}_B = P_E \Rightarrow \\
&\qquad \Rightarrow \omega_E \times (R_\Theta \mathrm{I}_B \omega_B) + R_\Theta \mathrm{I}_B \dot{\omega}_B = R_\Theta P_B \Rightarrow \\
&\qquad \Rightarrow R_\Theta(\omega_B \times (\mathrm{I}_B \omega_B)) + R_\Theta \mathrm{I}_B \dot{\omega}_B = R_\Theta P_B \Rightarrow \\
&\qquad \Rightarrow (\omega_B \times (\mathrm{I}_B \omega_B)) + \mathrm{I}_B \dot{\omega}_B = P_B \Rightarrow \\
&\qquad \Rightarrow -S(I_B \omega_B)\omega_B + \mathrm{I}_B \dot{\omega}_B = P_B
\end{aligned}$$

Therefore we have an expression for rotational dynamics in the B-frame. To summarize, the dynamics are enclosed in these two equations:

$$\begin{aligned}
&M_q x_E = F_E \\
&-S(I_B \omega_B)\omega_B + \mathrm{I}_B \dot{\omega}_B = P_B
\end{aligned}$$

or, written in the H-frame, they can be summed up in one equation:

$$M_H \dot{\zeta} + C_H(\zeta)\zeta = \begin{bmatrix} F_E \\ P_B \end{bmatrix} \quad (1.6)$$

where $M_H = \begin{bmatrix} M_q & 0 & 0 & 0 & 0 & 0 \\ 0 & M_q & 0 & 0 & 0 & 0 \\ 0 & 0 & M_q & 0 & 0 & 0 \\ 0 & 0 & 0 & I_{XX} & 0 & 0 \\ 0 & 0 & 0 & 0 & I_{YY} & 0 \\ 0 & 0 & 0 & 0 & 0 & I_{ZZ} \end{bmatrix}$ is the inertia matrix,

$C_H(\zeta) = \begin{bmatrix} 0_{3x3} & 0_{3x3} \\ 0_{3x3} & -S(I_B \omega_B) \end{bmatrix}$ is the centrifugal-coriolis matrix,

and F_E and P_B are outside forces and outside torques respectively. F_E is given by the sum of three terms, $F_E = G_E + Th_E + wF_E$:

- G_E is gravity:

$$G_E = \begin{bmatrix} 0 \\ 0 \\ -M_q g \end{bmatrix}$$

- Th_E is propeller thrust:

$$Th_E = R_\Theta U_1 = \begin{bmatrix} (\sin(\psi)\sin(\varphi) + \cos(\psi)\sin(\theta)\cos(\theta))\, U_1 \\ (-\cos(\psi)\sin(\varphi) + \sin(\psi)\sin(\theta)\cos(\varphi))\, U_1 \\ \cos(\theta)\cos(\varphi) U_1 \end{bmatrix}$$

  (U_1 is an input signal discussed in detail in the Appendix 5.2)

- wF_E any outside disturbances, like wind gusts:

$$wF_E = \begin{bmatrix} wF_{E,X} & wF_{E,Y} & wF_{E,Z} \end{bmatrix}^T$$

  While P_B is given by the sum $P_B = GE_B(\omega_B) + PT_B + wT_B$ where:

- The Gyroscopic Effect matrix (extensive explanation for the gyroscopic effect in subsection 5.3 of the Appendix)is:

$$GE_B(\omega_B) = J_{TP} \begin{bmatrix} q & -q & q & -q \\ -p & p & -p & p \\ 0 & 0 & 0 & 0 \end{bmatrix} \begin{bmatrix} \Omega_1 \\ \Omega_2 \\ \Omega_3 \\ \Omega_4 \end{bmatrix}$$

- $PT_B = \begin{bmatrix} U_2 & U_3 & U_4 \end{bmatrix}^T$ is the matrix containing the Propeller Torques (U_2, U_3, U_4 are the inputs discussed in detail in the Appendix 5.2) and

- $wT_B = \begin{bmatrix} wT_{B,p} & wT_{B,q} & wT_{B,r} \end{bmatrix}^T$ are any outside torques caused by disturbances like wind perturbations.

By expanding equation (1.6) for each coordinate we finally get the following dynamics for a quadrotor UAV:

$$\ddot{X} = (\sin(\psi)\sin(\varphi) + \cos(\psi)\sin(\theta)\cos(\varphi))\,\frac{U_1}{M_q} + \frac{wF_{E,x}}{M_q} \tag{1.7}$$

$$\ddot{Y} = (-\cos(\psi)\sin(\varphi) + \sin(\psi)\sin(\theta)\cos(\varphi))\,\frac{U_1}{M_q} + \frac{wF_{E,y}}{M_q} \tag{1.8}$$

$$\ddot{Z} = -g + (\cos(\theta)\cos(\varphi))\,\frac{U_1}{M_q} + \frac{wF_{E,z}}{M_q} \tag{1.9}$$

$$\dot{p} = \frac{I_{YY} - I_{ZZ}}{I_{XX}}qr - \frac{J_{TP}}{I_{XX}}q\Omega + \frac{U_2}{I_{XX}} + \frac{wT_{B,p}}{I_{XX}} \tag{1.10}$$

$$\dot{q} = \frac{I_{ZZ} - I_{XX}}{I_{YY}}pr + \frac{J_{TP}}{I_{YY}}p\Omega + \frac{U_3}{I_{YY}} + \frac{wT_{B,q}}{I_{YY}} \tag{1.11}$$

$$\dot{r} = \frac{I_{XX} - I_{YY}}{I_{ZZ}}pq + \frac{U_4}{I_{ZZ}} + \frac{wT_{B,r}}{I_{ZZ}} \tag{1.12}$$

But we are not done yet. There is a second factor, that plays an important role in a quadrotor's flight, and that is its motors' dynamics. The motors, being electrical circuits with inductive properties, have a complicated response to stimulating signals, that goes beyond a simple linear relationship between input and output. Their inductive properties factor in to their behaviour, but two other terms play the most prominent role. First is the Back EMF, a voltage created by the rotor's spinning, and second is the aerodynamic drag force exerted on the propellers. Back EMF voltage is proportional to the angular speed of the rotor and its polarity opposes that of the input voltage. Aerodynamic drag is proportional to rotational speed squared. All those factors summed together give us the following equation for the DC motors:

$$(J_P + \eta N^2 J_M)\dot{\Omega} = -\frac{\mathrm{K}_E K_M}{R}\eta N^2\Omega - d\Omega^2 + \frac{K_M}{R}\eta N u \tag{1.13}$$

where:
Ω: 4x1 vector containing angular speeds of the four motors.
u: 4x1 vector of voltages for the four motors
K_E, K_M: Motor specific constants.
R: Electrical Resistance
η: conversion efficiency
N: reduction ratio
d: air drag coefficient
J_P: moment of inertia about the propeller axis.
J_M: moment of inertia about the rotor axis.

Exactly how the previous equation is derived, can be found in [1].

Finally we can see a diagram of how the whole dynamics, rigid body and motors are interconnected to form the final Quadrotor Dynamics Block:

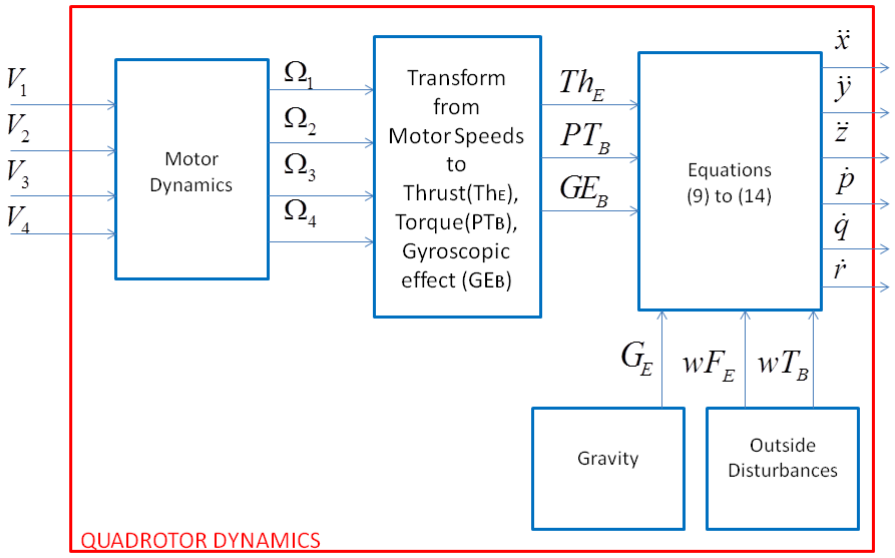

Fig. 1.2: Quadrotor Dynamics Diagram

.

We have managed to array a detailed, complete layout of a quadrotor's dynamics and their exact derivation starting from basic lagrangian mechanics. Before describing the control system used to stabilise the quadrotor, an analysis of why the quadrotor system is inherently unstable needs to be presented first. Such an analysis can convince that a control loop is essential for flying the vehicle stably, without having it perform uncontrollable and unpredictable movements. The theorem we'll be basing our analysis on is called the Intermediate Axis Theorem or, more recently, the Dzhanibekov Effect (named after a Russian astronaut who thought of a disturbing potential application of this theorem). As we've seen, the quadrotor has three principal axes , where moments of inertia around those form the diagonal elements of the moment of inertia matrix I_B when rotation is viewed in the B-frame. As we've seen this matrix is given as:

$$I_B = \begin{bmatrix} I_{XX} & 0 & 0 \\ 0 & I_{YY} & 0 \\ 0 & 0 & I_{ZZ} \end{bmatrix}$$

The geometry of the quadrotor dictates that I_{ZZ} is the largest of the three moments of inertia. Then for I_{YY} and I_{XX}, we theoretically consider them equal, but in practice true symmetry is impossible and many quadrotors have asymmetrical bodies, therefore we can assume that $I_{YY} \neq I_{XX}$. Because the quadcopter is a flying vehicle the slightest difference between I_{YY} and I_{XX} can have a huge impact on its stability. We now take

equations (1.10),(1.11),(1.12)

$$\dot{p} = \frac{I_{YY} - I_{ZZ}}{I_{XX}} qr - \frac{J_{TP}}{I_{XX}} q\Omega + \frac{U_2}{I_{XX}} + \frac{wT_{B,p}}{I_{XX}}$$
$$\dot{q} = \frac{I_{ZZ} - I_{XX}}{I_{YY}} pr + \frac{J_{TP}}{I_{YY}} p\Omega + \frac{U_3}{I_{YY}} + \frac{wT_{B,q}}{I_{YY}}$$
$$\dot{r} = \frac{I_{XX} - I_{YY}}{I_{ZZ}} pq + \frac{U_4}{I_{ZZ}} + \frac{wT_{B,r}}{I_{ZZ}}$$

For the sake of simplicity we consider any disturbance equal to zero ($wT_{B,p} = 0, wT_{B,q} = 0, wT_{B,r} = 0$). Moreover, we consider any inputs equal to zero: $U_2 = 0, U_3 = 0, U_4 = 0$ and the Gyroscopic Effect's influence equal to zero (without loss of generality): $\Omega = \Omega_1 - \Omega_2 + \Omega_3 - \Omega_4 = 0$ Therefore equations (1.10),(1.11),(1.12) become:

$$\dot{p} = \frac{I_{YY} - I_{ZZ}}{I_{XX}} qr$$
$$\dot{q} = \frac{I_{ZZ} - I_{XX}}{I_{YY}} pr$$
$$\dot{r} = \frac{I_{XX} - I_{YY}}{I_{ZZ}} pq$$

or written in Newton-Euler form:

$$\mathrm{I}_B \dot{\omega}_\mathrm{B} + \omega_\mathrm{B} \times (\mathrm{I}_B \omega_\mathrm{B}) = 0 \tag{1.14}$$

. Our strategy will be to linearise the previous equation around $\omega_B = \omega_s + a$ with

$$\omega_s = \begin{bmatrix} 0 \\ q_s \\ 0 \end{bmatrix}$$

and $a = \begin{bmatrix} a_p \\ a_q \\ a_r \end{bmatrix}$ being a divergence from ω_s. Thus equation (1.14) becomes:

$$\begin{aligned} \dot{a} &= -{I_B}^{-1} \left((\omega_s + a) \times (I_B \omega_s + I_B a) \right) = \\ &= -{I_B}^{-1} \left((\omega_s \times (I_B \omega_s) + \omega_s \times (I_B a) + a \times (I_B \omega_s + I_B a) \right) = \\ &= -{I_B}^{-1} \left((\omega_s \times (I_B a) + a \times (I_B \omega_s) + a \times (I_B a) \right) \end{aligned}$$

We throw away the second order term $a \times (I_B a)$, therefore getting the following linearised dynamics:

$$\dot{a} = -{I_B}^{-1} \left((\omega_s \times (I_B a) + a \times (I_B \omega_s) \right) = -{I_B}^{-1} A a$$

By doing the calculations matrix A equals:

$$A = \begin{pmatrix} 0 & 0 & (I_{ZZ} - I_{YY}) q_s \\ 0 & 0 & 0 \\ (I_{YY} - I_{XX}) q_s & 0 & 0 \end{pmatrix}$$

We need to determine the eigenvalues of matrix $-{I_B}^{-1}A$ to elaborate on the stability of the linear system:

$$\dot{a} = -{I_B}^{-1}Aa$$

The eigenvalue equation will be:

$$\det(\lambda I - (-{I_B}^{-1}Aa)) = \det \begin{pmatrix} \lambda & 0 & \frac{I_{ZZ} - I_{YY}}{\mathrm{I}_{XX}} q_s \\ 0 & \lambda & 0 \\ \frac{I_{YY} - I_{XX}}{I_{ZZ}} q_s & 0 & \lambda \end{pmatrix} \Rightarrow$$

$$\Rightarrow \lambda \left(\lambda^2 - \frac{{q_s}^2}{I_{ZZ} I_{XX}} (I_{YY} - I_{XX})(I_{ZZ} - I_{YY}) \right)$$

which give 3 different eigenvalues:

$$\begin{aligned} \lambda_1 &= 0 \\ \lambda_2 &= \sqrt{\frac{{q_s}^2}{I_{ZZ} I_{XX}} (I_{YY} - I_{XX})(I_{ZZ} - I_{YY})} \\ \lambda_3 &= -\sqrt{\frac{{q_s}^2}{I_{ZZ} I_{XX}} (I_{YY} - I_{XX})(I_{ZZ} - I_{YY})} \end{aligned} \tag{1.15}$$

For $I_{XX} < I_{YY} < I_{ZZ}$ we get three real eigenvalues with $\lambda_2 > 0$ and $\lambda_3 < 0$. Therefore rotation around the intermediate axis, Y-axis in our example, is a saddle point and, as such, it is unstable since any minor divergence(vector a in our example) causes exponential growth in the vehicle's angular velocity. More information can be found in [2].

How to control this heavily nonlinear system of intermingled states? Thankfully, there is a way and it's really simple. Just a PID controller. While the quadrotor has 6 degrees of freedom, the available input signals are four. The quadrotor is an underactuated system. We'll choose to control the three attitude coordinates as well as the altitude. By controlling the attitude, we'll form a second PID loop that controls the spatial X,Y coordinates by transforming desired X,Y to desired values for the Euler angles. Now let's analyse the first level of PID control, for attitude and altitude. By supposing that the quadrotor is always functioning close to being parallel with the ground, we take that $T_\Theta \simeq \mathrm{I}$ and therefore these assumptions can be made:

$$\begin{aligned} p &\simeq \dot{\phi} \\ q &\simeq \dot{\theta} \\ r &\simeq \dot{\psi} \\ \dot{p} &\simeq \ddot{\phi} \\ \dot{q} &\simeq \ddot{\theta} \\ \dot{r} &\simeq \ddot{\psi} \end{aligned} \tag{1.16}$$

By these assumptions equations (1.10),(1.11),(1.12) become:

$$\begin{aligned}\ddot{\phi} &= \frac{I_{YY}-I_{ZZ}}{I_{XX}}\dot{\theta}\dot{\psi} - \frac{J_{TP}}{I_{XX}}\dot{\theta}\cdot\Omega + \frac{U_2}{I_{XX}} + \frac{wT_{B,p}}{I_{XX}} \\ \ddot{\theta} &= \frac{I_{ZZ}-I_{XX}}{I_{YY}}\dot{\phi}\dot{\psi} + \frac{J_{TP}}{I_{YY}}\dot{\varphi}\cdot\Omega + \frac{U_3}{I_{YY}} + \frac{wT_{B,q}}{I_{YY}} \\ \ddot{\psi} &= \frac{I_{XX}-I_{YY}}{I_{ZZ}}\dot{\phi}\dot{\theta} + \frac{U_4}{I_{ZZ}} + \frac{wT_{B,r}}{I_{ZZ}}\end{aligned} \tag{1.17}$$

These equations are of the following form:

$$\begin{aligned}\dot{x}_1 &= x_2 \\ \dot{x}_2 &= f(x_1, x_2) + u\end{aligned} \tag{1.18}$$

where:

$$f(x_1,x_2) = \begin{bmatrix} \frac{I_{YY}-I_{ZZ}}{I_{XX}}\dot{\theta}\dot{\psi} - \frac{J_{TP}}{I_{XX}}\dot{\theta}\cdot\Omega + \frac{wT_{B,p}}{I_{XX}} \\ \frac{I_{ZZ}-I_{XX}}{I_{YY}}\dot{\phi}\dot{\psi} + \frac{J_{TP}}{I_{YY}}\dot{\phi}\cdot\Omega + \frac{wT_{B,q}}{I_{YY}} \\ \frac{I_{XX}-I_{YY}}{I_{ZZ}}\dot{\phi}\dot{\theta} + \frac{wT_{B,r}}{I_{ZZ}} \end{bmatrix} \tag{1.19}$$

and

$$x_1 = \begin{bmatrix} \phi \\ \theta \\ \psi \end{bmatrix}$$

. According to paper [3] a PID controller of general form:

$$u = k_p(x_1 - y^*) + k_d\frac{d(x_1-y^*)}{dt} + k_i\int_0^t (x_1-y^*)dt$$

with $y^* = \begin{bmatrix} \phi_d & \theta_d & \psi_d \end{bmatrix}^T$ being the vector of desired values, and k_p, k_i, k_d the gains multiplying the proportional, integral and derivative terms, can control this system and send x_1 to a desired value y^* if and only if:

$$\left\| \frac{df}{dx_1} \right\| < L_1$$

$$\left\| \frac{df}{dx_2} \right\| < L_2$$

$$\frac{df}{du} > \underline{b}\mathrm{I}$$

where $L_1, L_2, \underline{b}$ some arbitrary positive constants. Since disturbances wT have bounded derivatives with respect to x_1, x_2 (they are wind gusts after all), then the prerequisites of the theorem are fulfilled and thus PID control is enough to stabilise the system and drive its x_1 states to y^*. The four equations that will be controlled with PIDs will be:

$$
\begin{aligned}
\ddot{Z} &= -g + \frac{U_1}{M_q} \\
\ddot{\phi} &= \frac{I_{YY} - I_{ZZ}}{I_{XX}}\dot{\theta}\dot{\psi} - \frac{J_{TP}}{I_{XX}}\dot{\theta}\cdot\Omega + \frac{U_2}{I_{XX}} + \frac{wT_{B,p}}{I_{XX}} \\
\ddot{\theta} &= \frac{I_{ZZ} - I_{XX}}{I_{YY}}\dot{\phi}\dot{\psi} + \frac{J_{TP}}{I_{YY}}\dot{\varphi}\cdot\Omega + \frac{U_3}{I_{YY}} + \frac{wT_{B,q}}{I_{YY}} \\
\ddot{\psi} &= \frac{I_{XX} - I_{YY}}{I_{ZZ}}\dot{\phi}\dot{\theta} + \frac{U_4}{I_{ZZ}} + \frac{wT_{B,r}}{I_{ZZ}}
\end{aligned}
\tag{1.20}
$$

where the PID controllers are given by:

$$
\begin{aligned}
U_1 &= k_{p,\mathrm{Z}}(Z - Z_d) + k_{d,\mathrm{Z}}\frac{d(Z - Z_d)}{dt} + k_{i,\mathrm{Z}}\int_0^t (Z - Z_d)dt \\
U_2 &= k_{p,\varphi}(\varphi - \varphi_d) + k_{d,\varphi}\frac{d(\varphi - \varphi_d)}{dt} + k_{i,\varphi}\int_0^t (\varphi - \varphi_d)dt \\
U_3 &= k_{p,\theta}(\theta - \theta_d) + k_{d,\theta}\frac{d(\theta - \theta_d)}{dt} + k_{i,\theta}\int_0^t (\theta - \theta_d)dt \\
U_4 &= k_{p,\psi}(\psi - \psi_d) + k_{d,\psi}\frac{d(\psi - \psi_d)}{dt} + k_{i,\psi}\int_0^t (\psi - \psi_d)dt
\end{aligned}
$$

Now in order to complete the control loop we need to translate the inputs from torques to voltages, so we can feed them back to the quadrotor's motors. As explained in the Appendix subsection 5.2 of this thesis, the inputs as a function of motor speeds are given by:

$$
\begin{aligned}
U_1 &= b({\Omega_1}^2 + {\Omega_2}^2 + {\Omega_3}^2 + {\Omega_4}^2) \\
U_2 &= lb(-{\Omega_2}^2 + {\Omega_4}^2) \\
U_3 &= lb(-{\Omega_1}^2 + {\Omega_3}^2) \\
U_4 &= d(-{\Omega_1}^2 + {\Omega_2}^2 - {\Omega_3}^2 + {\Omega_4}^2)
\end{aligned}
$$

Solving those four equations for the motor speeds we get:

$$
\begin{aligned}
{\Omega_1}^2 &= \frac{1}{4b}U_1 - \frac{1}{2bl}U_3 - \frac{1}{4d}U_4 \\
{\Omega_2}^2 &= \frac{1}{4b}U_1 - \frac{1}{2bl}U_2 + \frac{1}{4d}U_4 \\
{\Omega_3}^2 &= \frac{1}{4b}U_1 + \frac{1}{2bl}U_3 - \frac{1}{4d}U_4 \\
{\Omega_4}^2 &= \frac{1}{4b}U_1 + \frac{1}{2bl}U_2 + \frac{1}{4d}U_4
\end{aligned}
\tag{1.21}
$$

Now those motor speeds need to be assigned each to a voltage value through the motor's equation (1.13). But as is, that equation is too complicated, therefore we'll simplify it by linearising it using first order Taylor expansion for a multiple variables function. This expansion is given by:

$$f(x,y) = f(x_0,y_0) + \left.\frac{df}{dx}\right|_{x_0,y_0}(x-x_0) + \left.\frac{df}{dy}\right|_{x_0,y_0}(y-y_0)$$

Therefore the equation will become:

$$\dot{\mathbf{\Omega}} = \mathrm{A}_p\mathbf{\Omega} + B_p v + C_p \tag{1.22}$$

where:

$$\mathbf{\Omega} = \begin{bmatrix} \Omega_1 \\ \Omega_2 \\ \Omega_3 \\ \Omega_4 \end{bmatrix}$$

$$A_p = \left.\frac{d\dot{\omega}_p}{d\omega_p}\right|_{\omega_p=\omega_H, v=0} = -K_E K_M \eta \frac{N}{J_{TP}R}^2 - \frac{2d}{J_{TP}}\omega_H$$

$$B_p = \left.\frac{d\dot{\omega}_p}{dv}\right|_{\omega_p=\omega_H, v=0} = \frac{K_M \eta N}{J_{TP}R}$$

$$C_p = \frac{d}{J_{TP}}{\omega_H}^2$$

Solving for the voltages v we finally get:

$$v = \begin{bmatrix} V_1 \\ V_2 \\ V_3 \\ V_4 \end{bmatrix} = (1/B_p)\left(\begin{bmatrix} \dot{\Omega}_1 \\ \dot{\Omega}_2 \\ \dot{\Omega}_3 \\ \dot{\Omega}_4 \end{bmatrix} - \mathrm{A}_p \begin{bmatrix} \Omega_1 \\ \Omega_2 \\ \Omega_3 \\ \Omega_4 \end{bmatrix} - C_p\right)$$

In figure 1.3 we see the whole altitude and attitude control loop:

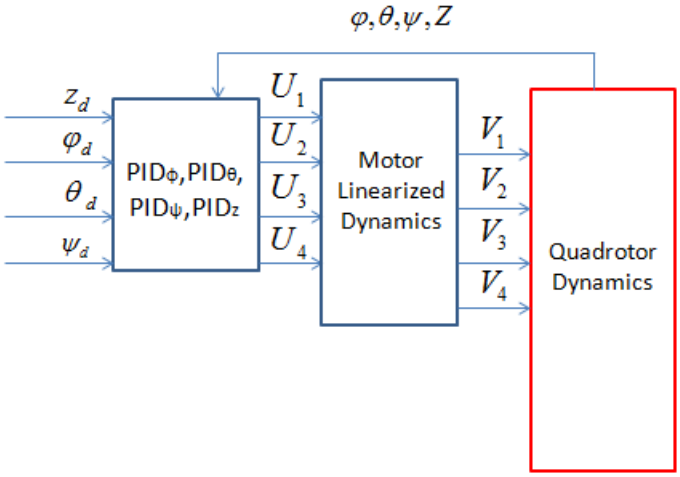

Fig. 1.3: Altitude and Attitude PID Control Scheme

Now it's time to address the second PID loop, for controlling the X,Y coordinates. This loop takes the X,Y desired feeds them to a PID loop and solves equations (1.7),(1.8)

with respect to ϕ, θ to determine desired angle values. Equations (1.7),(1.8) are:

$$\ddot{X} = (\sin(\psi)\sin(\phi) + \cos(\psi)\sin(\theta)\cos(\varphi))\frac{U_1}{M_q} + \frac{wF_{E,x}}{M_q} \quad (1.7)$$

$$\ddot{Y} = (-\cos(\psi)\sin(\phi) + \sin(\psi)\sin(\theta)\cos(\phi))\frac{U_1}{M_q} + \frac{wF_{E,y}}{M_q} \quad (1.8)$$

We want the accelerations of X,Y to follow a PID controller's commands, therefore:

$$\ddot{X} = k_{p,X}(X - X_d) + k_{d,X}\frac{d(X - X_d)}{dt} + k_{i,X}\int_0^t (X - X_d)dt = PID_X \quad (1.23)$$

$$\ddot{Y} = k_{p,Y}(Y - Y_d) + k_{d,Y}\frac{d(Y - Y_d)}{dt} + k_{i,Y}\int_0^t (Y - Y_d)dt = PID_Y \quad (1.24)$$

Thus, from equating (1.7),(1.8) and (1.23),(1.24) we get:

$$PID_X = (\sin(\psi_d)\sin(\phi_d) + \cos(\psi_d)\sin(\theta_d)\cos(\phi_d))\frac{U_1}{M_q} + \frac{wF_{E,x}}{M_q} = u_x$$

$$PID_Y = (-\cos(\psi_d)\sin(\phi_d) + \sin(\psi_d)\sin(\theta_d)\cos(\phi_d))\frac{U_1}{M_q} + \frac{wF_{E,y}}{M_q} = u_y$$

and solving for ϕ_d, θ_d we finally have:

$$\phi_d = asin(\frac{u_x\sin(\psi_d) - u_y\cos(\psi_d)}{U_1}) \quad (1.25)$$

$$\theta_d = asin(\frac{u_x\cos(\psi_d) + u_y\sin(\psi_d)}{U_1\cos(\phi_d)}) \quad (1.26)$$

The desired values X_d, Y_d, Z_d, ψ_d are generated by a trajectory block, that calculates and determines a trajectory for the vehicle, and gives out the trajectory's spatial coordinates X,Y,Z as the desired values for the quadrotor. Also the trajectory block generates the desired value for ψ, for the yaw of the quadrotor, thus we are able to control where the camera points at, for example.

The whole PID cascade control schematic can be seen in Figure 1.4

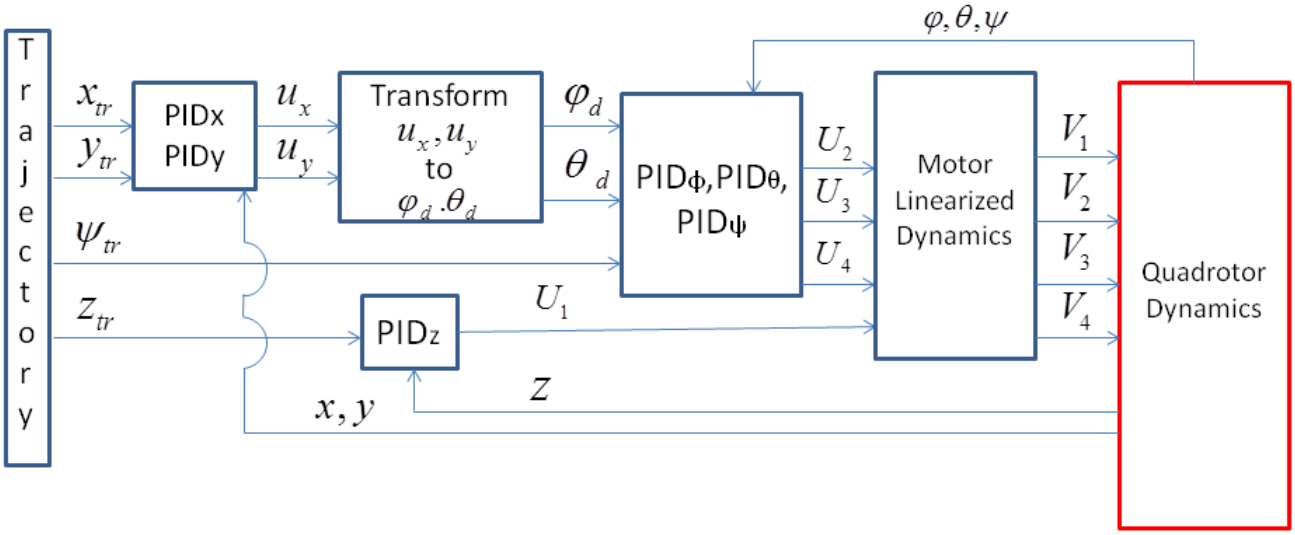

Fig. 1.4: PID-Cascade Schematic

2. DYNAMIC MODEL OF A QUADROTOR SLUNG-LOAD SYSTEM

In this section a detailed description will be given, of how the model of the quadrotor slung-load system was derived. There exists a thorough inspection of slung-load systems in reference [4]. In this thesis, the particular system of a quadrotor with a slung-load will be investigated, having followed the train of thought presented in the aforementioned paper. Problems of the slung-load type are mainly tackled in two different ways. Firstly, by considering the cable that holds the load as elastic, therefore that it has the properties of a spring, and secondly, by considering the cable to be rigid as a massless rod, therefore unchanging in length. The first approach consumes much less processing power during simulation, because the system's equations of motion are simpler than the equations derived through the second approach. Still, the first approach is not preferable as it inserts oscillations along the length of the cable which are not close to reality as a phenomenon. Therefore, this thesis proceeds with the second approach, theorising that the cable is a rigid massless rod that connects two bodies. So the cable acts as a holonomic constraint, restricting the movements of the second body, the load. This constraint will be taken account of during the planning of the systems generalised coordinates.

So, in order to derive the model the Lagrangian of the system needs to be determined. The system is made out of a rigid body, the quadrotor, which has 6 degrees of freedom, the load which is taken as a point mass thus having three degrees of freedom, and the cable which introduces the holonomic constraint.

As we've seen, the quadrotor's position of its centre-mass in the E-frame is given by vector

$$X_{cm} = \begin{bmatrix} X \\ Y \\ Z \end{bmatrix}$$

From Figure 2.1, the pendulum's position in the E-frame is given by vector X_{pen} :

$$X_{pen} = X_{cm} + R_{\Theta} \begin{bmatrix} a \\ b \\ \zeta + r_{pen} \end{bmatrix} \tag{2.1}$$

where $R_{\Theta} = \begin{bmatrix} c_\psi c_\phi & -s_\psi c_\phi + c_\psi s_\theta s_\phi & s_\psi s_\phi + c_\psi s_\theta c_\phi \\ s_\psi c_\theta & c_\psi c_\phi + s_\psi s_\theta s_\phi & -c_\psi s_\phi + s_\psi s_\theta c_\phi \\ -s_\theta & s_\phi c_\theta & c_\phi c_\theta \end{bmatrix}$

is the rotation matrix resulting from the sequence of Euler angle rotations. a, b, ζ are the coordinates of the pendulum expressed in the body-fixed frame of reference and $\begin{bmatrix} 0 & 0 & r_{pen} \end{bmatrix}^T$ is the position of the point from which the pendulum is fixed on the quadrotor, again expressed in B-frame. Two assumptions are made at this moment. First,

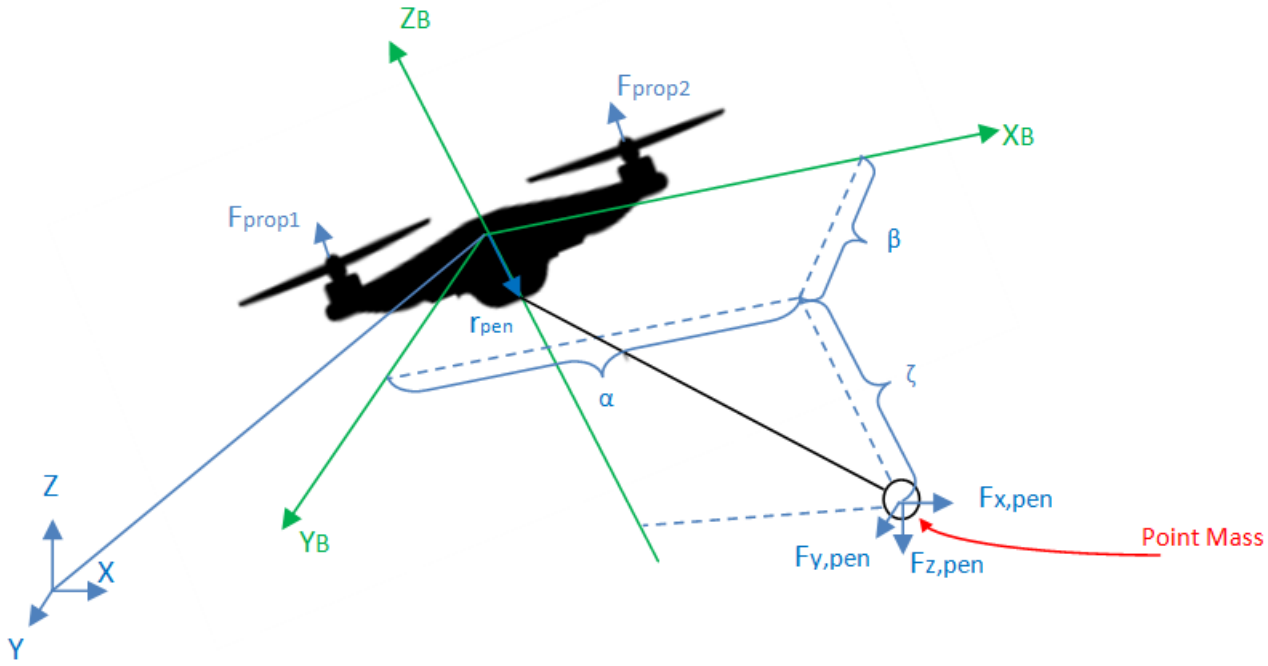

Fig. 2.1: Schematic of the Quadrotor Slung-Load System

the pendulum can never have a positive ζ and second the cable has a constant length, which is the holonomic constraint. These two assumptions give us: $\zeta = -\sqrt{L^2 - a^2 - b^2}$ and substituting it in (2.1) we finally get:

$$X_{pen} = X_{cm} + R_{\Theta} \begin{bmatrix} a \\ b \\ -\sqrt{L^2 - a^2 - b^2} + r_{pen} \end{bmatrix}$$

The vector of velocities expressed in the E-frame is then defined as:

$$u = \begin{bmatrix} \dot{X} \\ \dot{Y} \\ \dot{Z} \\ \dot{x}_{pen} \\ \dot{y}_{pen} \\ \dot{z}_{pen} \\ p \\ q \\ r \end{bmatrix}$$

and the vector of generalised coordinates is defined as :

$$q = \begin{bmatrix} X \\ Y \\ Z \\ a \\ b \\ \phi \\ \theta \\ \psi \end{bmatrix}$$

We'll draw a connection between the vectors q and u. The time derivative of the pendulum's position is given as:

$$\dot{X}_{pen} = \begin{bmatrix} \dot{x}_{pen} \\ \dot{y}_{pen} \\ \dot{z}_{pen} \end{bmatrix} = \dot{X}_{cm} + \dot{R}_{\Theta} \begin{bmatrix} a \\ b \\ -\sqrt{L^2 - a^2 - b^2} \end{bmatrix} + R_{\Theta} \begin{bmatrix} \dot{a} \\ \dot{b} \\ \frac{a\dot{a} + b\dot{b}}{\sqrt{L^2 - a^2 - b^2}} \end{bmatrix}$$

As we've seen angular speed in the body frame is:

$$\omega_B = \begin{bmatrix} p \\ q \\ r \end{bmatrix}$$

We can define the following relationship between the time derivatives of Euler angles $\dot{\Theta}_I = \begin{bmatrix} \dot{\phi} & \dot{\theta} & \dot{\psi} \end{bmatrix}^T$ and ω_B : $\omega_B = \mathrm{T}_{\Theta}^{-1} \dot{\Theta}_I$

$$\text{with } \mathrm{T}_{\Theta}^{-1} = \begin{bmatrix} 1 & 0 & -\sin\theta \\ 0 & \cos\phi & \cos\theta\sin\phi \\ 0 & -\sin\phi & \cos\phi\cos\theta \end{bmatrix}$$

The two vectors u and q are connected by matrix A according to the relation:

$$u = A\dot{q}$$

where matrix A is the Jacobian of vector u with respect to $\dot{q}$, therefore having the following form:

$$A = \frac{du}{d\dot{q}} = \begin{bmatrix} \frac{d\dot{X}}{d\dot{X}} & \frac{d\dot{X}}{d\dot{Y}} & \frac{d\dot{X}}{d\dot{Z}} & \frac{d\dot{X}}{d\dot{\alpha}} & \frac{d\dot{X}}{d\dot{\beta}} & \frac{d\dot{X}}{d\dot{\phi}} & \frac{d\dot{X}}{d\dot{\theta}} & \frac{d\dot{X}}{d\dot{\psi}} \\ \frac{d\dot{\Upsilon}}{d\dot{X}} & \frac{d\dot{\Upsilon}}{d\dot{Y}} & \frac{d\dot{\Upsilon}}{d\dot{Z}} & \frac{d\dot{\Upsilon}}{d\dot{\alpha}} & \frac{d\dot{\Upsilon}}{d\dot{\beta}} & \frac{d\dot{\Upsilon}}{d\dot{\phi}} & \frac{d\dot{\Upsilon}}{d\dot{\theta}} & \frac{d\dot{\Upsilon}}{d\dot{\psi}} \\ \frac{d\dot{Z}}{d\dot{X}} & \frac{d\dot{Z}}{d\dot{Y}} & \frac{d\dot{Z}}{d\dot{Z}} & \frac{d\dot{Z}}{d\dot{\alpha}} & \frac{d\dot{Z}}{d\dot{\beta}} & \frac{d\dot{Z}}{d\dot{\phi}} & \frac{d\dot{Z}}{d\dot{\theta}} & \frac{d\dot{Z}}{d\dot{\psi}} \\ \frac{d\dot{x}_{pen}}{d\dot{X}} & \frac{d\dot{x}_{pen}}{d\dot{Y}} & \frac{d\dot{x}_{pen}}{d\dot{Z}} & \frac{d\dot{x}_{pen}}{d\dot{\alpha}} & \frac{d\dot{x}_{pen}}{d\dot{\beta}} & \frac{d\dot{x}_{pen}}{d\dot{\phi}} & \frac{d\dot{x}_{pen}}{d\dot{\theta}} & \frac{d\dot{x}_{pen}}{d\dot{\psi}} \\ \frac{d\dot{y}_{pen}}{d\dot{X}} & \frac{d\dot{y}_{pen}}{d\dot{Y}} & \frac{d\dot{y}_{pen}}{d\dot{Z}} & \frac{d\dot{y}_{pen}}{d\dot{\alpha}} & \frac{d\dot{y}_{pen}}{d\dot{\beta}} & \frac{d\dot{y}_{pen}}{d\dot{\phi}} & \frac{d\dot{y}_{pen}}{d\dot{\theta}} & \frac{d\dot{y}_{pen}}{d\dot{\psi}} \\ \frac{d\dot{z}_{pen}}{d\dot{X}} & \frac{d\dot{z}_{pen}}{d\dot{Y}} & \frac{d\dot{z}_{pen}}{d\dot{Z}} & \frac{d\dot{z}_{pen}}{d\dot{\alpha}} & \frac{d\dot{z}_{pen}}{d\dot{\beta}} & \frac{d\dot{z}_{pen}}{d\dot{\phi}} & \frac{d\dot{z}_{pen}}{d\dot{\theta}} & \frac{d\dot{z}_{pen}}{d\dot{\psi}} \\ \frac{dp}{d\dot{X}} & \frac{dp}{d\dot{Y}} & \frac{dp}{d\dot{Z}} & \frac{dp}{d\dot{\alpha}} & \frac{dp}{d\dot{\beta}} & \frac{dp}{d\dot{\phi}} & \frac{dp}{d\dot{\theta}} & \frac{dp}{d\dot{\psi}} \\ \frac{dq}{d\dot{X}} & \frac{dq}{d\dot{Y}} & \frac{dq}{d\dot{Z}} & \frac{dq}{d\dot{\alpha}} & \frac{dq}{d\dot{\beta}} & \frac{dq}{d\dot{\phi}} & \frac{dq}{d\dot{\theta}} & \frac{dq}{d\dot{\psi}} \\ \frac{dr}{d\dot{X}} & \frac{dr}{d\dot{Y}} & \frac{dr}{d\dot{Z}} & \frac{dr}{d\dot{\alpha}} & \frac{dr}{d\dot{\beta}} & \frac{dr}{d\dot{\phi}} & \frac{dr}{d\dot{\theta}} & \frac{dr}{d\dot{\psi}} \end{bmatrix} =$$

$$= \begin{bmatrix} 1 & 0 & 0 & & & & & \\ 0 & 1 & 0 & & & 0_{3x5} & & \\ 0 & 0 & 1 & & & & & \\ \frac{d\dot{x}_{pen}}{d\dot{X}} & \frac{d\dot{x}_{pen}}{d\dot{Y}} & \frac{d\dot{x}_{pen}}{d\dot{Z}} & \frac{d\dot{x}_{pen}}{d\dot{\alpha}} & \frac{d\dot{x}_{pen}}{d\dot{\beta}} & \frac{d\dot{x}_{pen}}{d\dot{\phi}} & \frac{d\dot{x}_{pen}}{d\dot{\theta}} & \frac{d\dot{x}_{pen}}{d\dot{\psi}} \\ \frac{d\dot{y}_{pen}}{d\dot{X}} & \frac{d\dot{y}_{pen}}{d\dot{Y}} & \frac{d\dot{y}_{pen}}{d\dot{Z}} & \frac{d\dot{y}_{pen}}{d\dot{\alpha}} & \frac{d\dot{y}_{pen}}{d\dot{\beta}} & \frac{d\dot{y}_{pen}}{d\dot{\phi}} & \frac{d\dot{y}_{pen}}{d\dot{\theta}} & \frac{d\dot{y}_{pen}}{d\dot{\psi}} \\ \frac{d\dot{z}_{pen}}{d\dot{X}} & \frac{d\dot{z}_{pen}}{d\dot{Y}} & \frac{d\dot{z}_{pen}}{d\dot{Z}} & \frac{d\dot{z}_{pen}}{d\dot{\alpha}} & \frac{d\dot{z}_{pen}}{d\dot{\beta}} & \frac{d\dot{z}_{pen}}{d\dot{\phi}} & \frac{d\dot{z}_{pen}}{d\dot{\theta}} & \frac{d\dot{z}_{pen}}{d\dot{\psi}} \\ & & & & & & & \\ & 0_{3x5} & & & & T_{\Theta}{}^{-1} & & \\ & & & & & & & \end{bmatrix}$$

Now we define vector f_g, which contains the forces of gravity and vector f_a which contains the forces of thrust and of the gyroscopic effect acting on the quadrotor as well as any outside forces acting on the system such as wind and water drag. The sum of all outside forces acting on the quadrotor including thrust U_1, wind gusts on the X,Y,Z axis are denoted as F_x, F_y, F_z accordingly. Similarly, the sum of all outside forces acting on the pendulum including wind or water drag on the X,Y,Z axis are denoted as $F_{x,pen}, F_{y,pen}, F_{z,pen}$ .The sum of torques around X axis of the B-frame including input torques U_2, U_3, U_4, gyroscopic effect and wind turbulations are denoted as P_x^B and so on for y and z.

$$f_g = \begin{bmatrix} 0 \\ 0 \\ -M_q g \\ 0 \\ 0 \\ -m_{pen} g \\ 0 \\ 0 \\ 0 \end{bmatrix} \qquad f_a = \begin{bmatrix} F_x \\ F_y \\ F_z \\ F_{x,pen} \\ F_{y,pen} \\ F_{z,pen} \\ \mathrm{P}_x^B \\ \mathrm{P}_y^B \\ \mathrm{P}_z^B \end{bmatrix}$$

Moreover, we define the inertia matrix D, a diagonal matrix containing the quadrotor mass (M_q) , the pendulum mass (m_{pen}) and the moments of inertia for X_B,Y_B,Z_B axis of the body frame:

$$D = \begin{bmatrix} M_q & 0 & 0 & 0 & 0 & 0 & 0 & 0 & 0 \\ 0 & M_q & 0 & 0 & 0 & 0 & 0 & 0 & 0 \\ 0 & 0 & M_q & 0 & 0 & 0 & 0 & 0 & 0 \\ 0 & 0 & 0 & m_{pen} & 0 & 0 & 0 & 0 & 0 \\ 0 & 0 & 0 & 0 & m_{pen} & 0 & 0 & 0 & 0 \\ 0 & 0 & 0 & 0 & 0 & m_{pen} & 0 & 0 & 0 \\ 0 & 0 & 0 & 0 & 0 & 0 & Ixx & 0 & 0 \\ 0 & 0 & 0 & 0 & 0 & 0 & 0 & Iyy & 0 \\ 0 & 0 & 0 & 0 & 0 & 0 & 0 & 0 & Izz \end{bmatrix}$$

The translational kinetic energy of the quadrotor's center of mass will be:

$$KE_{q,tr} = \frac{1}{2} \begin{bmatrix} \dot{X} \\ \dot{Y} \\ \dot{Z} \end{bmatrix}^T \begin{bmatrix} M_q & 0 & 0 \\ 0 & M_q & 0 \\ 0 & 0 & M_q \end{bmatrix} \begin{bmatrix} \dot{X} \\ \dot{Y} \\ \dot{Z} \end{bmatrix}$$

As for the quadrotor rotational kinetic energy we can use relation (1.4) to express E-frame kinetic energy to B-frame kinetic energy:

$$\begin{aligned} KE_{q,rot,E} &= \frac{1}{2} {\omega_E}^T I_E \omega_E = \frac{1}{2} (R_\Theta \omega_B)^T I_E (R_\Theta \omega_B) = \\ &= \frac{1}{2} (R_\Theta \omega_B)^T I_E (R_\Theta \omega_B) = \frac{1}{2} {\omega_B}^T ({R_\Theta}^T I_E R_\Theta) \omega_B = \\ &= \frac{1}{2} {\omega_B}^T I_B \omega_B \end{aligned}$$

While the kinetic energy of the pendulum with respect to the inertial frame is:

$$KE_{pen,tr} = \frac{1}{2} \begin{bmatrix} \dot{x}_{pen} \\ \dot{y}_{pen} \\ \dot{z}_{pen} \end{bmatrix}^T \begin{bmatrix} M_q & 0 & 0 \\ 0 & M_q & 0 \\ 0 & 0 & M_q \end{bmatrix} \begin{bmatrix} \dot{x}_{pen} \\ \dot{y}_{pen} \\ \dot{z}_{pen} \end{bmatrix}$$

By summing up all the kinetic energies together we get the kinetic energy of the system:

$$KE = KE_{q,tr} + KE_{pen,tr} + KE_{q,rot} = \ = (1/2) u^T D u = (1/2) \dot{q}^T A^T D A \dot{q} \qquad (2.2)$$

Applying the Euler-Lagrange equation to (2.2) for every generalized coordinate gives us the following equation:

$$M(q)\ddot{q} + k(q,\dot{q}) = Q \tag{2.3}$$

where:

$$M = A^T D A \tag{2.4}$$
$$k = A^T D \dot{A}\dot{q} + (\dot{A} - G)^T D A \dot{q} \tag{2.5}$$
$$Q = A^T (f_a + f_g) \tag{2.6}$$

with G being the Jacobian of vector $A(q)\dot{q}$ with respect to q, given as $G = \nabla_q{}^T (A(q)\dot{q})$ and Q the vector of generalised forces. (Detailed proof of (2.3) in Appendix 5.4)
To make apparent the influence of the inputs on our system we analyse f_a as follows:

$$f_a = \begin{bmatrix} F_x \\ F_y \\ F_z \\ F_{x,pen} \\ F_{y,pen} \\ F_{z,pen} \\ \mathrm{P}^B_x \\ \mathrm{P}^B_y \\ \mathrm{P}^B_z \end{bmatrix} = \begin{bmatrix} 0 \\ 0 \\ 0 \\ F_{x,pen} \\ F_{y,pen} \\ F_{z,pen} \\ \mathrm{P}^B_{x,gyro} \\ \mathrm{P}^B_{y,gyro} \\ \mathrm{P}^B_{z,gyro} \end{bmatrix} + \begin{bmatrix} (\sin\psi\sin\phi + \cos\psi\sin\theta\cos\phi) & 0 & 0 & 0 \\ (-\cos\psi\sin\phi + \sin\psi\sin\theta\cos\phi) & 0 & 0 & 0 \\ \cos\theta\cos\phi & 0 & 0 & 0 \\ 0 & 0 & 0 & 0 \\ 0 & 0 & 0 & 0 \\ 0 & 0 & 0 & 0 \\ 0 & 1 & 0 & 0 \\ 0 & 0 & 1 & 0 \\ 0 & 0 & 0 & 1 \end{bmatrix} \begin{bmatrix} U_1 \\ U_2 \\ U_3 \\ U_4 \end{bmatrix} = S + W \cdot U \tag{2.7}$$

From relation (2.7) we can substitute the new expression for f_a to derive following result for the second time derivative of q:

$$\begin{aligned} \ddot{q} &= (A^T D A)^{-1}(Q - A^T D \dot{A}\dot{q} - (\dot{A} - G)^T D A \dot{q}) \\ &= (A^T D A)^{-1}(A^T(f_g + S) - A^T D \dot{A}\dot{q} - (\dot{A} - G)^T D A \dot{q}) + (A^T D A)^{-1} A^T W \cdot U \end{aligned} \tag{2.8}$$

To bring the system in the familiar form of a system with some unknown nonlinear dynamics $f(q,\dot{q})$ and some input U multiplied by a known nonlinear function $g(q,\dot{q})$ we define the following equations:

$$\begin{aligned} f(q,\dot{q}) &= (A^T D A)^{-1}(A^T(f_g + S) - A^T D \dot{A}\dot{q} - (\dot{A} - G)^T D A \dot{q}) \\ g(q,\dot{q}) &= (A^T D A)^{-1} A^T W \end{aligned}$$

Note that the unknown vector S (because it contains the outside disturbances of wind and water stream) is part of $f(q,\dot{q})$. That's why $f(q,\dot{q})$ is the unknown factor.
and substituting to equation (2.8) we have the final form for our system:

$$\ddot{q} = f(q,\dot{q}) + g(q,\dot{q})U \tag{2.9}$$

3. ACTIVE DISTURBANCE REJECTION CONTROL: THEORY AND APPLICATION

For almost a century proportional-integral-derivative(PID) has been the primary control law used in industry and all sorts of applications. Its first important advantage is being simple to tune, the technician only having to experiment with three different parameters, the gains that multiply the proportional, the integral and the derivative terms. Its second advantage is its robustness. As a control law that does not rely on the mathematical model of the plant but instead on its error output to act, PID can be applied to almost every control problem, and react to all sorts of uncertainties in contrast to a model based approach which is computationally intensive and has little room to account for uncertain terms in the dynamics. Moreover with PID being system agnostic we do not need to measure any parameter of the system such as mass or moment of inertia, in order to derive the control law. Control engineers have been looking to dethrone PID for a long time. Numerous ways have been devised to control systems that usually do a much better job than PID in terms of performance, but they lack its simplicity and its robustness. A new method was proposed by Han [7] that would supposedly revolutionise the industry, by replacing PID with a better, more robust overall controller, the Active Disturbance Rejection Controller. The idea of this new method was to measure the output of a system and with these measurements, using an observer to estimate its states, cancel the disturbances of the system and turn it into a cascade integrator form.In theory, ADRC offers all that PID offers, with the cost of being slightly more computation intensive. An example of this methodology follows.

Suppose we have the n-th order system of form:

$$\begin{aligned} \dot{x}_1 &= x_2 \\ \dot{x}_2 &= x_3 \\ &\vdots \\ \dot{x}_n &= f(x_1, ..., x_n) + w + g(x_1, ..., x_n)u \end{aligned} \tag{3.1}$$

where $f(x_1, ..., x_n)$ are the dynamics, w is an unknown disturbance, $g(x_1, ..., x_n)$ a function of the states and u the scalar input. We rewrite (3.1) as:

$$\begin{aligned} \dot{x}_1 &= x_2 \\ \dot{x}_2 &= x_3 \\ &\vdots \\ \dot{x}_n &= f(x_1, ..., x_n) + w + (g(x_1, ..., x_n) - b_0)u + b_0 u \end{aligned} \tag{3.2}$$

where b_0 is a tunable constant.

Then, denoting

$$\begin{aligned}
&f(x_1,...,x_n)+w+(g(x_1,...,x_n)-b_0)u=x_{n+1}\\
&\dot{x}_{n+1}=h(x_1,...,x_n)\\
&b=g(x_1,...,x_n)
\end{aligned}$$

the system (3.2) can be transformed to an extended system of n-th-plus-one order:

$$\begin{aligned}
&\dot{x}_1=x_2\\
&\dot{x}_2=x_3\\
&\quad\vdots\\
&\dot{x}_n=\dot{x}_{n+1}+b_0u\\
&\dot{x}_{n+1}=h(x_1,...,x_n)
\end{aligned}\tag{3.3}$$

We define the Extended State Observer of the system as

$$\begin{aligned}
&\dot{\hat{x}}_1=x_2\\
&\dot{\hat{x}}_2=\hat{x}_3-G_1(\hat{x}_1-x_1)\\
&\quad\vdots\\
&\dot{\hat{x}}_n=\hat{x}_{n+1}-G_{n-1}(\hat{x}_1-x_1)+b_0u\\
&\dot{\hat{x}}_{n+1}=-G_n(\hat{x}_1-x_1)
\end{aligned}$$

where $\hat{x}_1,\hat{x}_2,...,\hat{x}_{n+1}$ are the observed values by the ESO for states $x_1,x_2,...,x_{n+1}$, $G_1,G_2,...,G_n$ are linear or nonlinear functions of the difference $x_1-\hat{x}_1$.
By choosing as input:

$$u=\frac{u_0-\hat{x}_{n+1}}{b_0}$$

where $u_0=k_1(r-\hat{x}_1)+k_2(r-\hat{x}_2)+...+k_n(r^{(n)}-\hat{x}_n)$ the extended system from form (3.3) becomes:

$$\begin{aligned}
&x_1=x_2\\
&\quad\vdots\\
&\dot{x}_n=x_n-\hat{x}_n+k_1(r-\hat{x}_1)+k_2(\dot{r}-\hat{x}_2)+....+k_n(r^{(n)}-\hat{x}_n)
\end{aligned}$$

Taking for the extended state observer values that $x_1\approx\hat{x}_1,x_2\approx\hat{x}_2,...,x_n\approx\hat{x}_n$ the initial system takes the following form:

$$\begin{bmatrix}\dot{x}_1\\ \dot{x}_2\\ \vdots\\ \dot{x}_n\end{bmatrix}=\begin{bmatrix}0&1&0&\dots&0\\ 0&0&1&\dots&0\\ &\vdots&&&\\ 0&0&0&\dots&1\\ -k_1&-k_2&-k_3&\dots&-k_n\end{bmatrix}\begin{bmatrix}x_1\\ x_2\\ \vdots\\ x_n\end{bmatrix}+\begin{bmatrix}0&0&\dots&0\\ &\vdots&&\\ -k_1&-k_2&\dots&-k_n\end{bmatrix}\begin{bmatrix}r\\ \dot{r}\\ \vdots\\ r^{(n)}\end{bmatrix}$$

For x_1 to tend to r, $k_1,k_2,...,k_n$ need to be chosen so that matrix

$$\begin{bmatrix}0&1&0&\dots&0\\ 0&0&1&\dots&0\\ &\vdots&&&\\ 0&0&0&\dots&1\\ -k_1&-k_2&-k_3&\dots&-k_n\end{bmatrix}$$

is Hurwitz.

What the previous small application of ADRC shows, is that by measuring just the output x_1 we can form an observer dubbed the Extended State Observer (ESO) that estimates every state of the system even providing an estimation for unknown dynamics and disturbances ($\hat{x}_3$ in our example). By subtracting this estimation in our control law we can "cancel" the unknown terms and transform the system into the canonical cascade integrator form. The "" around cancel are there because an estimation cannot really cancel the disturbances it estimates, but it can severely mitigate their influence on the dynamics. Explicit theoretical proof for ADRC stability is hard to come by. In paper [8] we find the proof of stability for ADRCs using Linear Extended State Observers. That means there is proof of stability if the functions $G_1, G_2, ..., G_n$ we saw earlier in the example are linear functions of the error $(x_1 - \hat{x_1})$ e.g. $G_1 = \beta_1(x_1 - \hat{x_1})$,$G_2 = \beta_2(x_1 - \hat{x_1})$,...,$G_n = \beta_n(x_1 - \hat{x_1})$. Unfortunately, when these G functions become nonlinear, proving the stability of the ESO is much more difficult. These papers have proven it for a specific class of MIMO uncertain nonlinear systems([9],[10])

So the advantages of ADRC are:

1) Small to no reliance on the mathematical model of the plant, meaning the scheme of the controller is simpler and the transient response is satisfactory.
2) Can deal with almost every kind of uncertainty, meaning it's more robust.
3) Small number of parameters to tune.

3.1 Application on the Quadrotor Slung-Load System

As we saw earlier the quadrotor slung-load system dynamics are given by:

$$\ddot{q} = \begin{bmatrix} \ddot{X} \\ \ddot{Y} \\ \ddot{Z} \\ \ddot{a} \\ \ddot{b} \\ \ddot{\phi} \\ \ddot{\theta} \\ \ddot{\psi} \end{bmatrix} = f(q, \dot{q}) + g(q, \dot{q})U$$

where

$$f(q, \dot{q}) = (A^T D A)^{-1}(A^T(f_g + S) - A^T D \dot{A}\dot{q} - (\dot{A} - G)^T D A \dot{q})$$
$$g(q, \dot{q}) = (A^T D A)^{-1} A^T W$$

Second derivatives of Euler angle coordinates ϕ, θ, ψ and altitude Z can be written as:

$$\begin{bmatrix} \ddot{\phi} \\ \ddot{\theta} \\ \ddot{\psi} \\ \ddot{Z} \end{bmatrix} = \begin{bmatrix} f_1 \\ f_2 \\ f_3 \\ f_4 \end{bmatrix} + \begin{bmatrix} g_1 & 0 & 0 & 0 \\ 0 & g_2 & 0 & 0 \\ 0 & 0 & g_3 & 0 \\ 0 & 0 & 0 & g_4 \end{bmatrix} \begin{bmatrix} U_2 \\ U_3 \\ U_4 \\ U_1 \end{bmatrix}$$

where f_1, f_2, f_3, f_4 are unknown nonlinear functions and g_1, g_2, g_3, g_4 are the unknown nonlinear factors that multiply $U_2, U_3, U_4, U1$ respectively.

An ADRC can be created for each coordinate. Each coordinate is described by a second order system of form:

$$\begin{aligned} \dot{x}_1 &= x_2 \\ \dot{x}_2 &= f(x_1, x_2) + w + g(x_1, x_2)u \end{aligned} \tag{3.4}$$

where x_1, x_2 are the states with x_1 representing any of the four coordinates ϕ, θ, ψ, Z and x_2 the coordinate's time derivative. $f(x_1, x_2)$ represent the unknown nonlinear dynamics, w an unknown disturbance, and $g(x_1, x_2)$ the unknown nonlinear term that multiplies the input u. Paper [11] proves that a system like (3.4) can have its second state x_2 follow a desired value $x_{2,d}$, using an ADRC controller. By taking the second equation of (3.4) and rebranding terms:

$$\begin{aligned} &f(x_1, x_2) + w + (g(x_1, x_2)u - b_0 u) = x_3 \\ &b = g(x_1, x_2) \\ &\dot{x}_3 = h(t) \end{aligned}$$

we have the extended system for state x_2 :

$$\begin{aligned} \dot{x}_2 &= x_3 + b_0 u \\ \dot{x}_3 &= h(t) \end{aligned} \tag{3.5}$$

For this new system (3.5) we can build an Extended State Observer with the following form:

$$\begin{aligned} \dot{\hat{x}}_2 &= \hat{x}_3 - \beta_1(\hat{x}_2 - x_2) + b_0 u \\ \dot{\hat{x}}_3 &= -\beta_2(\hat{x}_2 - x_2) \end{aligned}$$

where $\hat{x}_2, \hat{x}_3$ are the estimations for states x_2, x_3, and β_1, β_2, b_0 positive tunable constants. Then according to paper [11] it can be proven that this Extended State Observer or ESO, can ensure the convergence of $\hat{x}_2, \hat{x}_3$ to x_2, x_3. Now, by choosing a control law u as:

$$u = (-k_1(\hat{x}_2 - x_2) - \hat{x}_3)/b_0$$

with k_1 being another tunable positive constant system (3.5) becomes:

$$\begin{aligned} \dot{x}_2 &= x_3 - \hat{x}_3 - k_1(\hat{x}_2 - x_2) \\ \dot{x}_3 &= h(t) \end{aligned}$$

In the same paper, it is proven that this control law forces x_2 to $x_{2,d}$. We can see intuitively how that might be by considering that $x_3 \simeq \hat{x}_3$. Then x_3 is "cancelled" and all that remains from the system is:

$$\dot{x}_2 = -k_1(\hat{x}_2 - x_2)$$

which stabilises x_2 and forces it to converge to $x_{2,d}$

In this way the velocity of the system converges to a desired velocity. But we want to control position x_1, not velocity. To achieve position control we build an outside loop PD such as the desired velocity $x_{2,d}$ is determined by the desired position $x_{1,d}$ as:

$$x_{2,d} = k_2 \left[(x_1 - x_{1,d}) + T_d \frac{d}{dt}(x_1 - x_{1,d}) \right]$$

where k_2 and T_d are positive tunable constants. Again in paper [11] it is proven that putting this outside PD loop just before the inner ADRC loop any system similar to a quadrotor (therefore even a quadrotor slung-load system) can have its state x_1 converge to a desired value $x_{1,d}$.

In the following figure we can see the dual loop PD-ADRC for angle control.

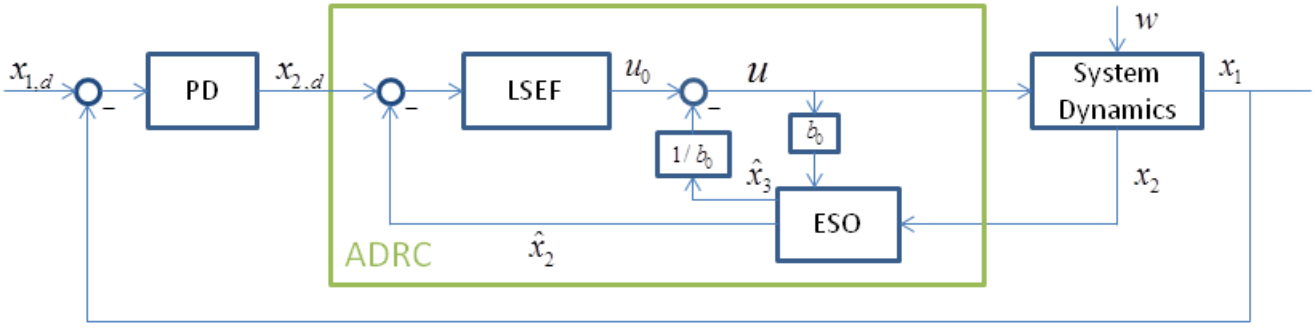

Fig. 3.1: PD-ADRC Scheme

- PD=Proportional Derivatve: Takes the difference $x_1 - x_{1,d}$ as input and gives as output the desired velocity according to equation:

$$x_{2,d} = k_2 \left[(x_1 - x_{1,d}) + T_d \frac{d}{dt}(x_1 - x_{1,d}) \right]$$

- LESO=Linear Extended State Observer: The observer that generates the estimated states as

$$\dot{\hat{x}}_2 = \hat{x}_3 - \beta_1(\hat{x}_2 - x_2) + b_0 u$$
$$\dot{\hat{x}}_3 = -\beta_2(\hat{x}_2 - x_2)$$

- LSEF=Linear State Error Feedback: Generates the control law as following:

$$u_0 = -k_1(\hat{x}_2 - x_2)/b_0$$

.

- System Dynamics: Self-explanatory!

As is, the PD-ADRC controller we have proposed has six gains in need of tuning: $k_1, k_2, T_d, b_0, \beta_1, \beta_2$ in contrast with a normal PID which has three. But, as seen in reference [8], ESO gains β_1, β_2 can be set equal to $[\beta_1, \beta_2] = [2\omega_0, {\omega_0}^2]$ where ω_0 is called the observer bandwidth. This transforms the characteristic polynomial of the ESO $s^2 + \beta_1 s + \beta_2$ as follows:

$$s^2 + \beta_1 s + \beta_2 = s^2 + 2\omega_0 s + {\omega_0}^2 = (s + \omega_0)^2$$

, therefore to a polynomial with only a double pole at position $-\omega_0$. The convergence rate of the whole ESO can now be controlled just by tuning ω_0. So we have managed to reduce the tunable constants of the PD-ADRC from six to five: $k_1, Td, k_2, b_0, \omega_0$, two more than the normal PID controller.

In figure 12 we can see the whole scheme of the Quadrotor Slung Load System using the dual loop PD-ADRC controller described previously.

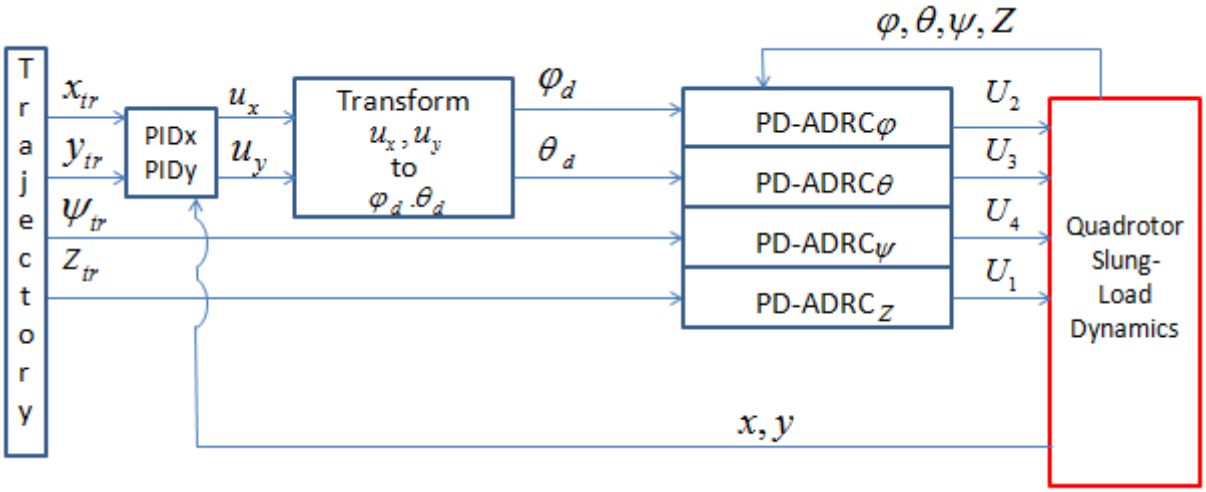

Fig. 3.2: Complete Scheme

Box Descriptions:

- Trajectory: Generates $x_{tr}, y_{tr}, z_{tr}, \psi_{tr}$ that we want the quadrotor to follow.
- PIDx,PIDy: They generate the u_x, u_y as:

$$u_x = k_{p_1}(x_{tr} - x) - k_{d1}\dot{x} + k_{I1}\int_0^t (x_{tr} - x)$$
$$u_y = k_{p_1}(y_{tr} - y) - k_{d1}\dot{y} + k_{I1}\int_0^t (y_{tr} - y)$$

- Transforming u_x, u_y to $\phi_d.\theta_d$ according to equations:

$$\phi_d = a\sin(u_x \sin(\psi_{tr}) - u_y \cos(\psi_{tr}))$$
$$\theta_d = a\sin(\frac{u_x \cos(\psi_d) + u_y \sin(\psi_d)}{\cos\phi_d})$$

- PD-ADRCφ,PD-ADRCθ,PD-ADRCψ,PD-ADRCz: The PD-ADRC scheme as it was described previously, for each of the three angles and the altitude Z.
- Dynamics: The dynamics of the quadrotor slung-load system.

4. SIMULATION RESULTS

In this section an extended analysis of the results of the simulations will be given. The proposed PD-ADRC controller will be tested and have its performance compared with the normal PID controller. At first stage, the performance of the two controllers will be evaluated at the level of angles, by turning off the PIDx and PIDy and setting a target angle for the controllers to reach. At second stage the PIDx, PIDy will be turned back on and two types of tests will be made to judge the performance of the complete system. The first will be a set-point test, in which the quadrotor slung-load system will be asked to stabilise on a position in 3D space some centimeters away from its initial position. The second test will be trajectory tracking, with increasing levels of noise applied to the euler angles equations. The w in system (3.4) will be the band limited white noise signal. Therefore a different white noise signal will be applied to each euler angle. The idea here is that the noise signal can model any noise inherent in the system's sensors or any wind gust turbulations. Moreover in all tests, aerodynamic drag will be exerted on the quadrotor's frame and we will consider that the load is submerged in water, thus having hydrostatic drag exerted on it from the water's current. As figure 4.1 demonstrates, there are forces acting on the load that need to be determined, namely the buoyancy and the hydrodynamic drag, as both weight and tension are known and considered in the system's modelling. By considering the load as a smooth sphere of radius of 5 cm ,for the sake of simplicity, then buoyancy is given by equation:

$$B = V\rho g$$

where $V = \frac{4}{3}\pi r^3 = 5,23 \cdot 10^{-4}\, m^3$ is the volume of the sphere, $\rho = 987\ kg/m^3$ is the water's density, and $g = 9.8\ m/s^2$ gravitational acceleration. While hydrodynamic drag is given by:

$$D_{water} = \frac{1}{2} C_d \rho A |u_{fluid} - u_{body}|(u_{fluid} - u_{body}) \tag{4.1}$$

where the drag coefficient is $C_d = 0.4$ because of the consideration that the load is a smooth sphere, $\rho = 987,\ kg/m^3$ is the water's density, and $A = \pi r^2 = 3.14 \cdot 0.0025\ m^2$ is the projection of the sphere on the surface perpendicular to the current flow of the fluid. Correspondingly, the expression giving the aerodynamic drag on the quadrotor body is:

$$D_{air} = K|u_{fluid} - u_{body}|(u_{fluid} - u_{body}) \tag{4.2}$$

where aerodynamic drag coefficient for a quadrotor, K ,is equal to 0.01 as per reference [11].

The quadrotor's mass, principal moments of inertia as well as all aerodynamic and propeller constants, are the same as those in [1], and are arrayed in detail in Appendix subsection 5.6. For the following tests the wind gust has a velocity of $u_{wind} = 3.5 +$

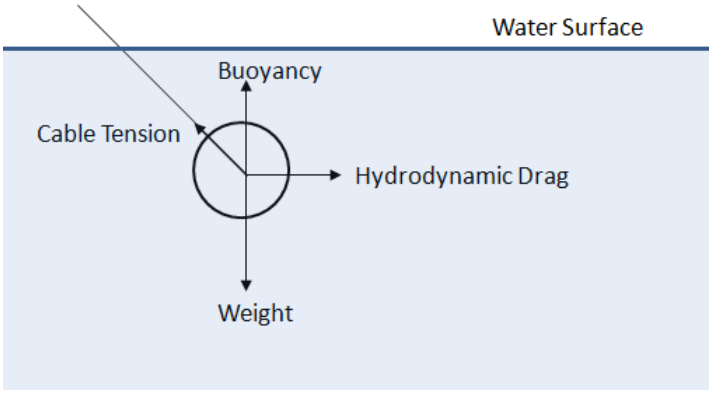

Fig. 4.1: Forces acting on Load

$0.01sin(0.04t) + 0.08sin(0.1t)$ m/s and direction (in spherical coordinates) $\varphi_{wind} = 30^o + 5^o \cdot sin(t) + 3^o \cdot sin(0.03t), \theta_{wind} = 45^o$ while the water current has a speed of $u_{water} = 0.7 + 0.01sin(3t) + 0.08sin(0.1t)$ m/s and direction (again in spherical coordinates) $\varphi_{water} = 30^o + 5^o \cdot sin(0.05t) + 3^o \cdot sin(0.1t), \theta_{water} = 90^o$.

4.1 Angle Set-point Test

By turning off control in the X,Y coordinates we can evaluate the performance of the PD-ADRC in terms of how fast it reaches the desired angle, and how well it eliminates disturbances. Considering that the load is dipped in the water at the 10 second time point, these are the produced graphs for the target angles of $\phi = 0.04$ rad , $\theta = 0$ rad and $\psi = 0$ rad:

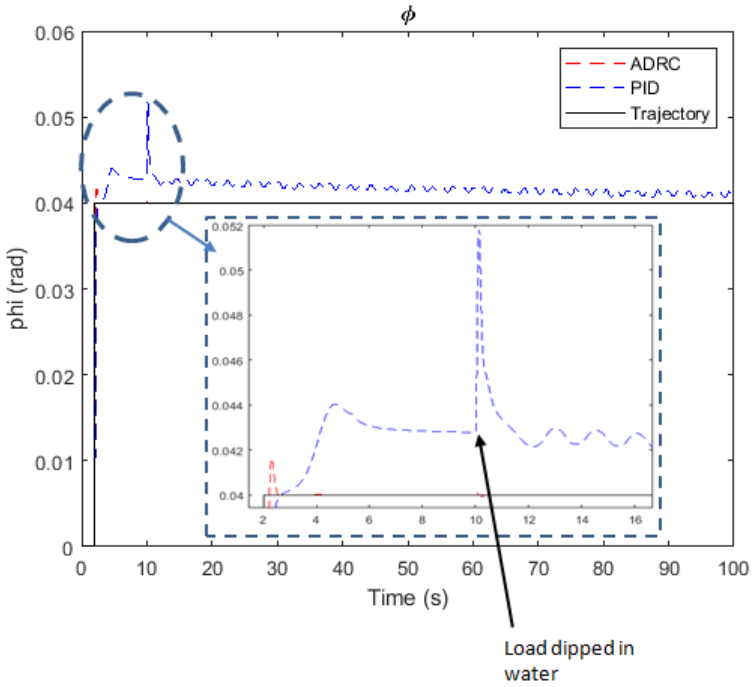

Fig. 4.2: phi for 0.04 rad setpoint

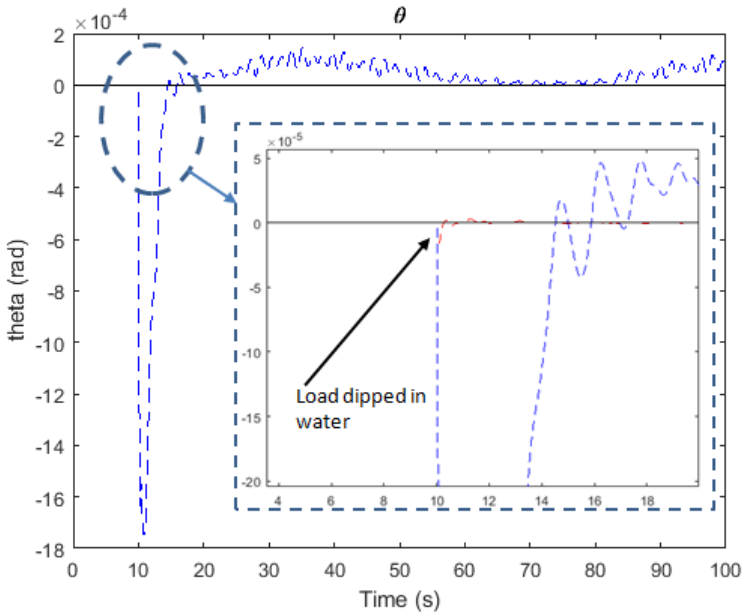

Fig. 4.3: theta for 0.04 rad setpoint

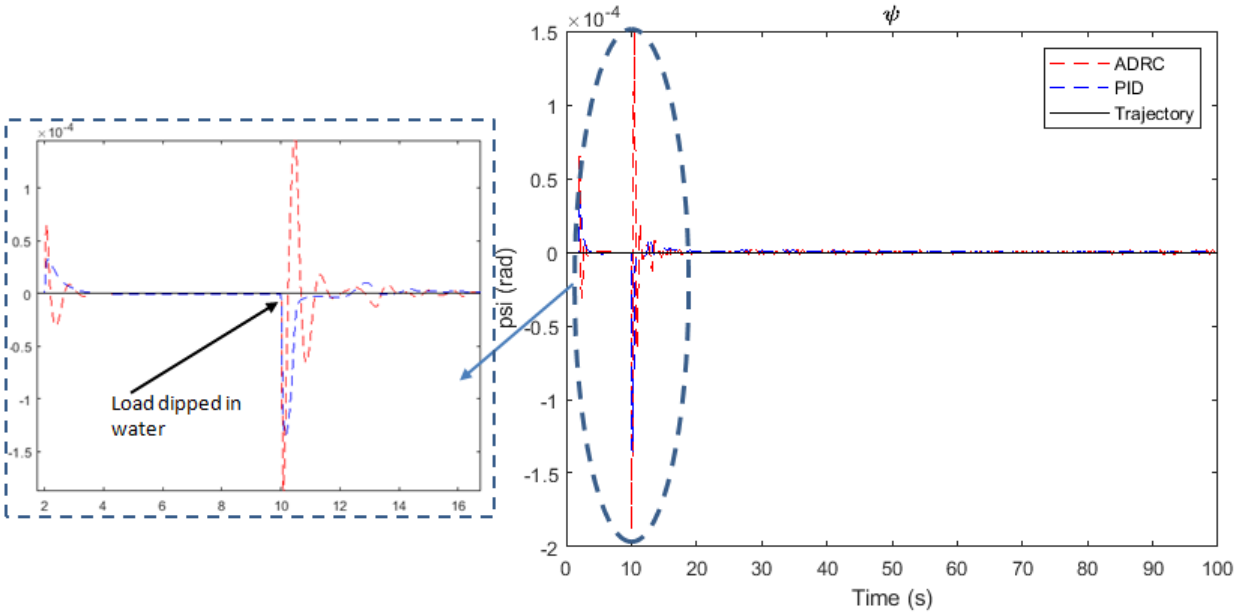

Fig. 4.4: psi for 0.04 rad setpoint

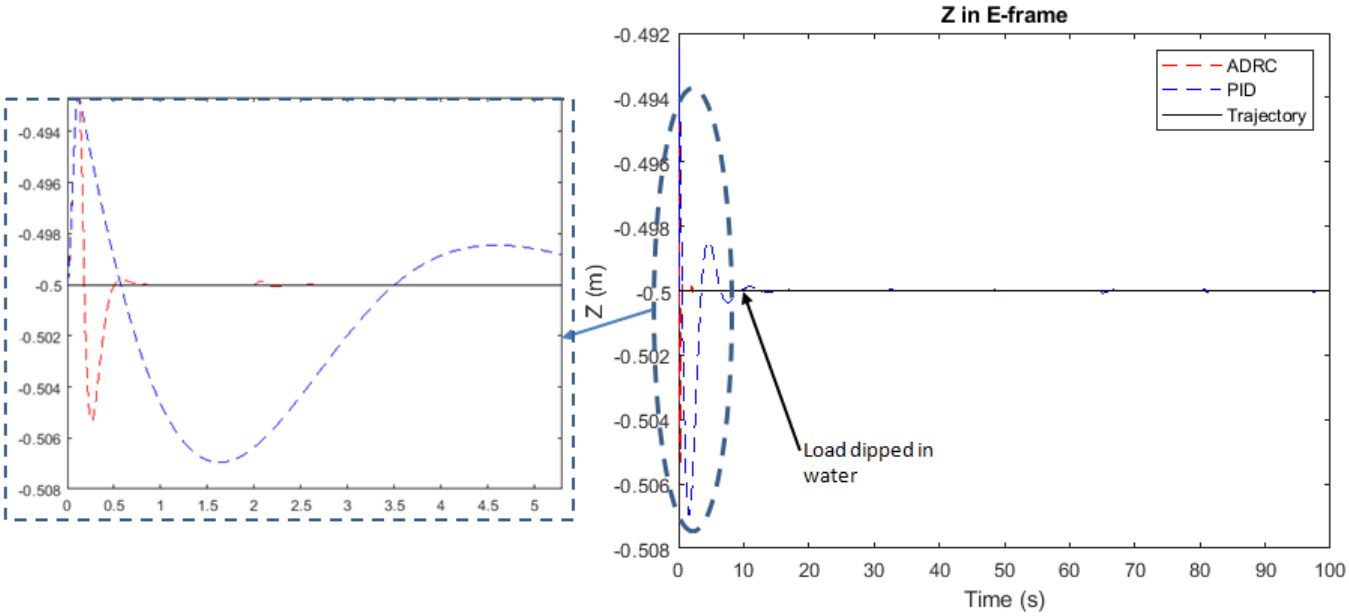

Fig. 4.5: Z for 0.04 rad setpoint

Changing the desired ϕ angle to 0.4 rad , produces the following graphs:

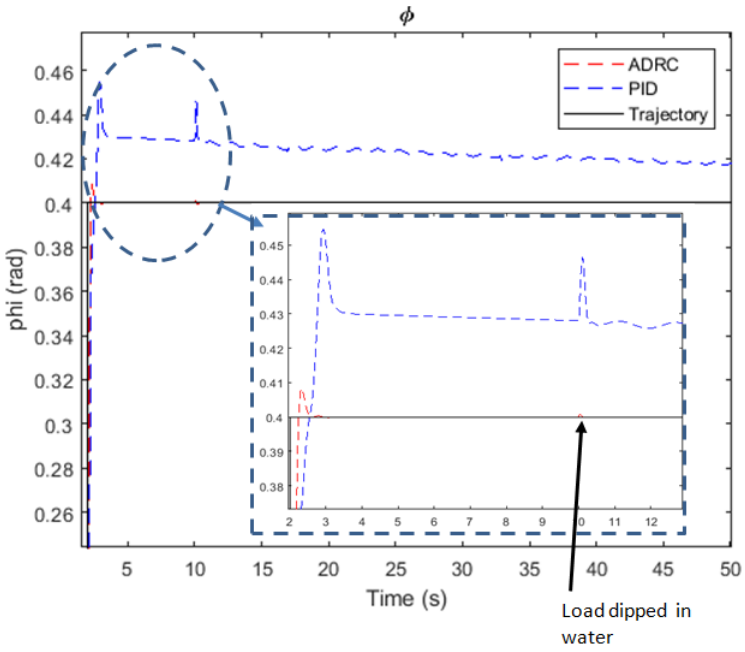

Fig. 4.6: phi for 0.4 rad setpoint

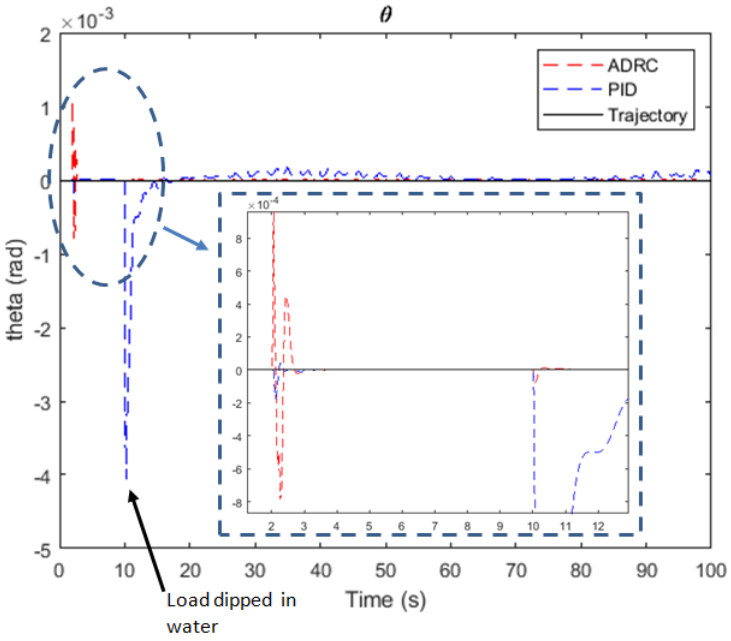

Fig. 4.7: theta for 0.4 rad setpoint

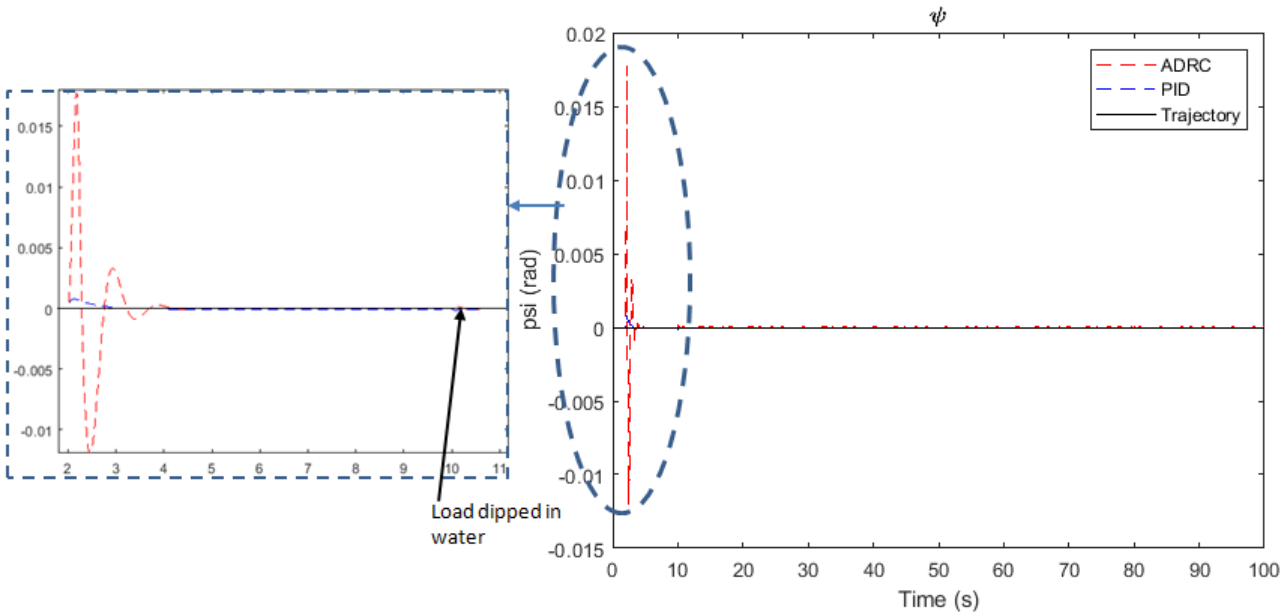

Fig. 4.8: psi for 0.4 rad setpoint

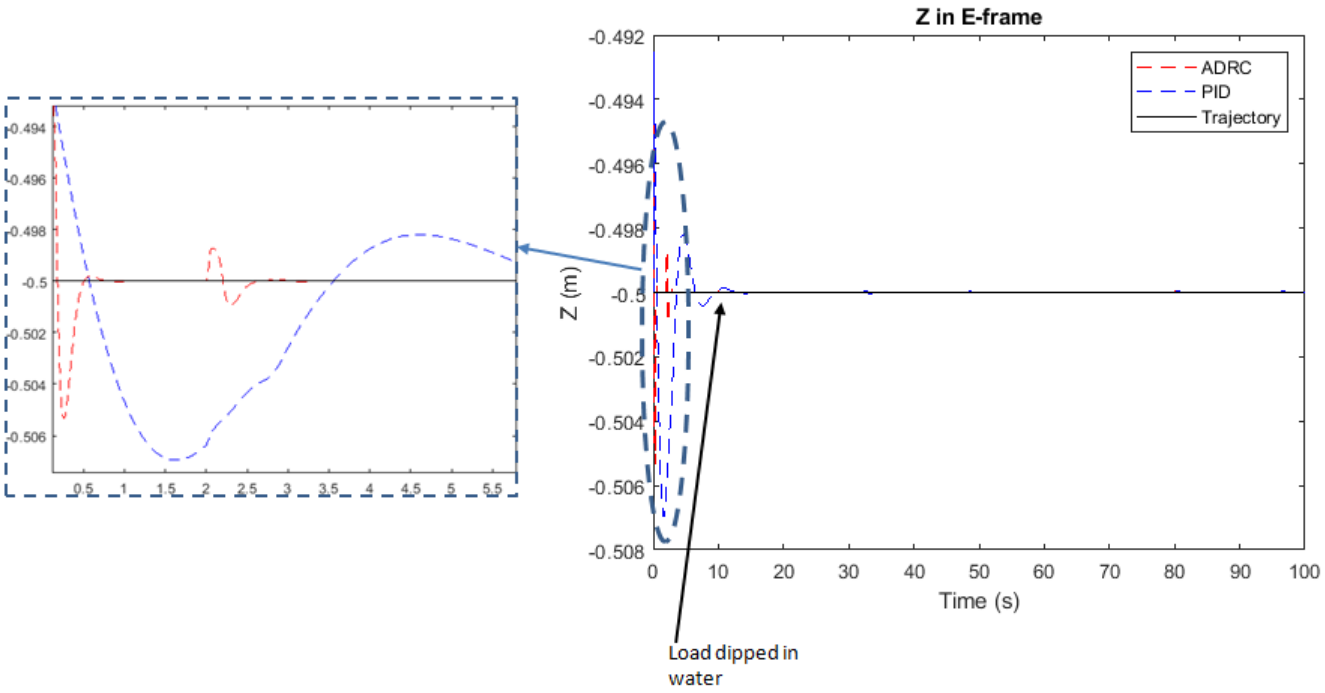

Fig. 4.9: Z for 0.4 rad setpoint

From the previous results, we can safely reach the conclusion that the PD-ADRC does a better job at following the desired ϕ angle, but is somewhat weaker in following the desired value (0 rad) for θ and ψ. In addition, it is much better at rejecting the water current disturbance on every coordinate except *psi*. In the following section we'll test the complete system, by turning on the PIDx, and PIDy controllers.

4.2 Spatial Set-point Test

This test involves setting a point in 3D space for the quadrotor slung-load system to go to and evaluating the resulting coordinate graphs. Aerodynamic drag and hydrodynamic drag start to affect the system at the 12 seconds time point. The test was made for the set-point of $(X_{tr}, Y_{tr}, Z_{tr}) = (0.1\ m, 0\ m, 0\ m)$ initially, then for $(X_{tr}, Y_{tr}, Z_{tr}) = (0.3\ m, 0\ m, 0\ m)$ and finally for $(X_{tr}, Y_{tr}, Z_{tr}) = (0.4\ m, 0\ m, 0\ m)$ The resulting graphs are arrayed below:

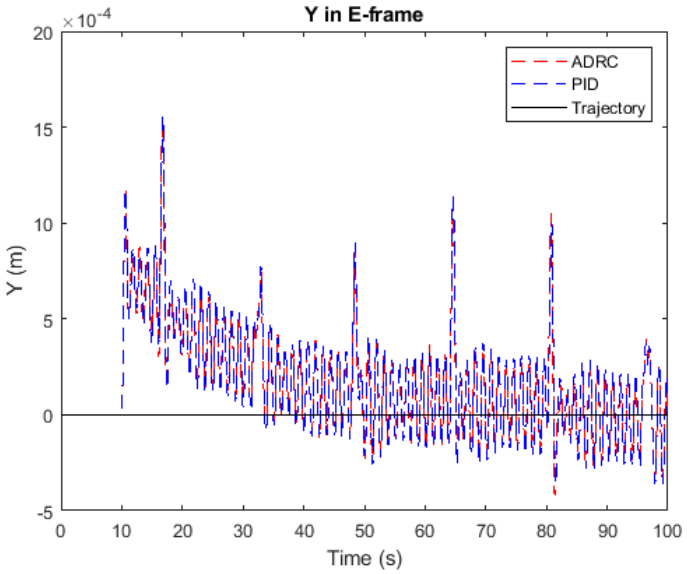

Fig. 4.10: Y for 0.1 setpoint

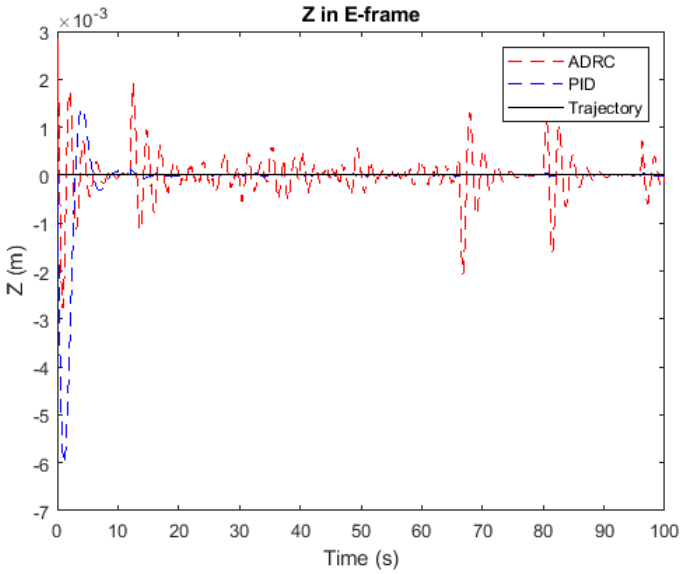

Fig. 4.11: Z for 0.1 setpoint

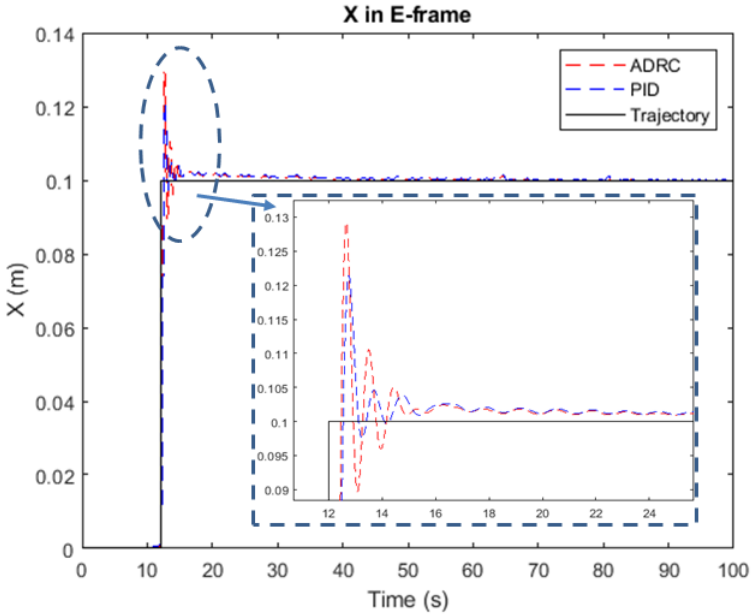

Fig. 4.12: X for 0.1 setpoint

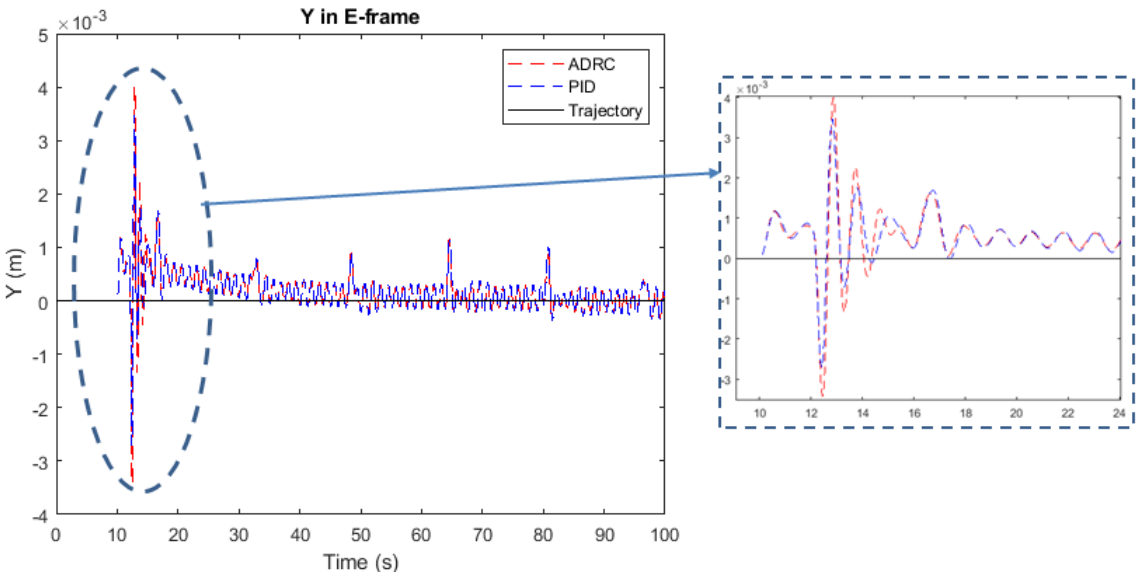

Fig. 4.13: Y for 0.3 setpoint

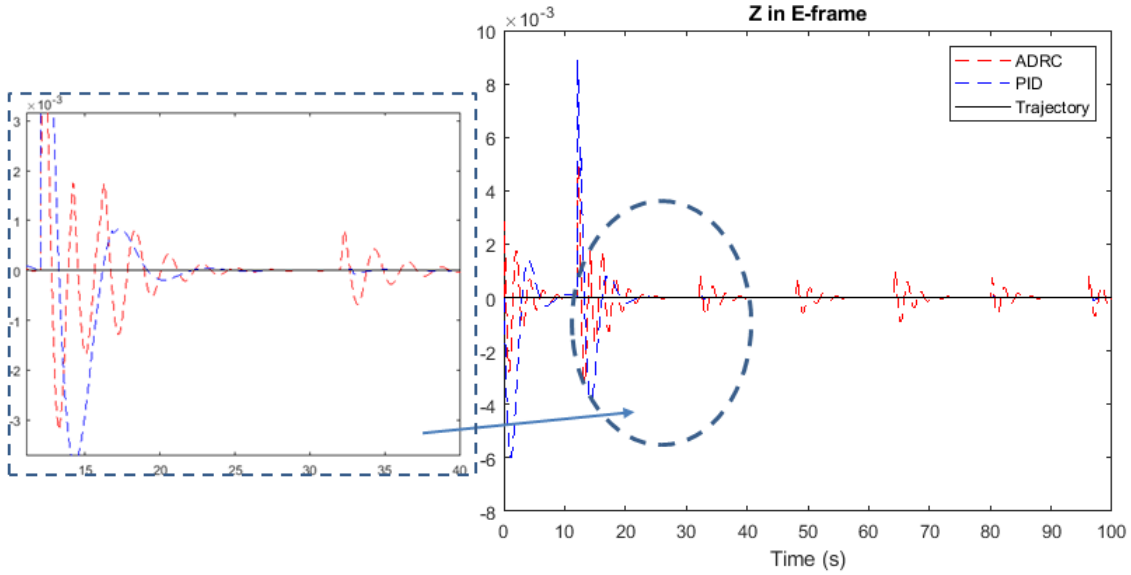

Fig. 4.14: Z for 0.3 setpoint

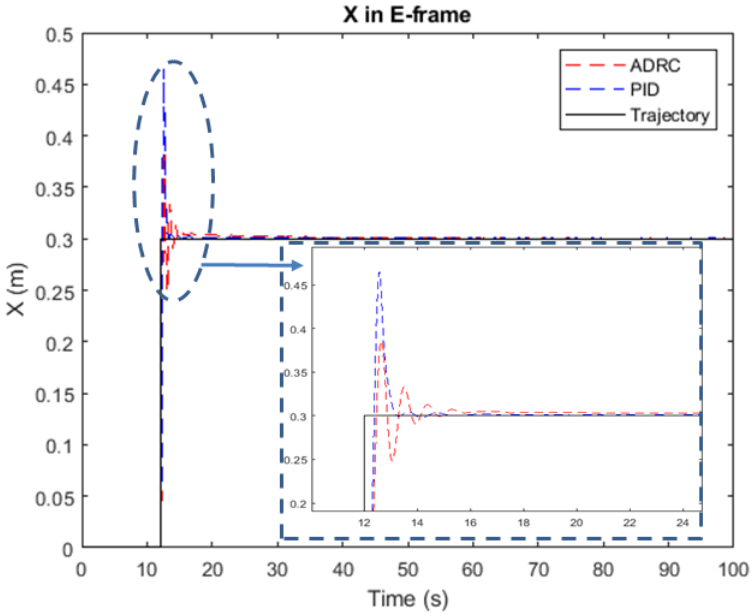

Fig. 4.15: X for 0.3 setpoint

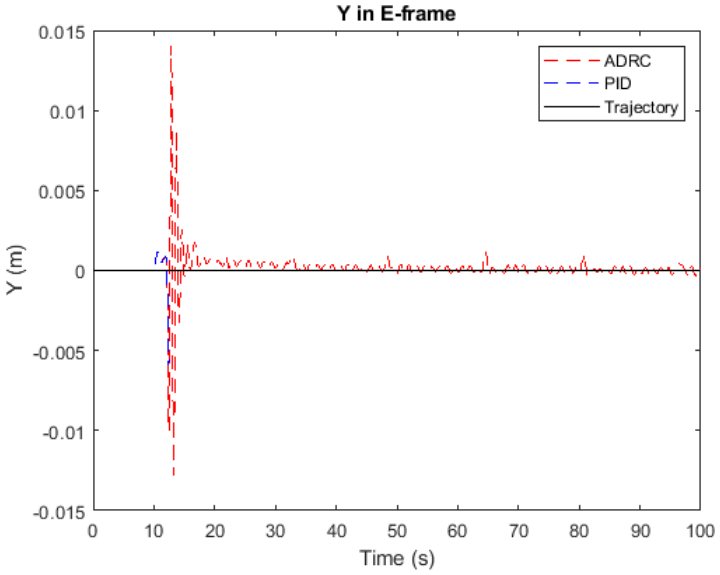

Fig. 4.16: Y for 0.4 setpoint

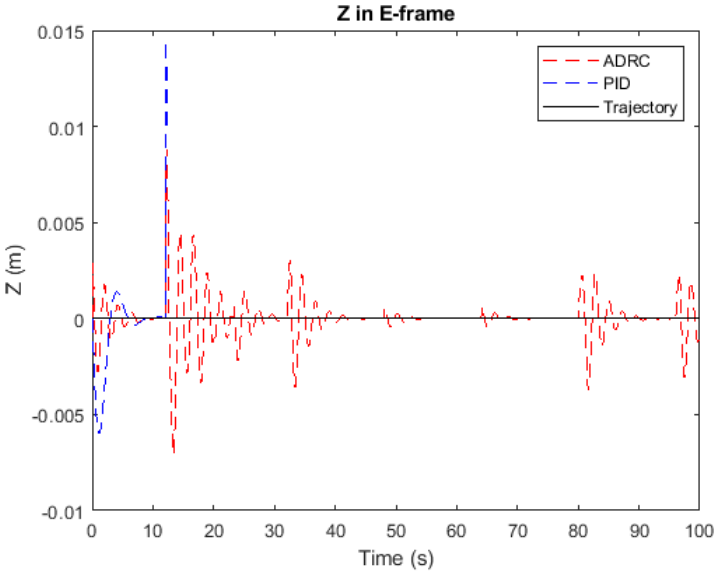

Fig. 4.17: Z for 0.4 setpoint

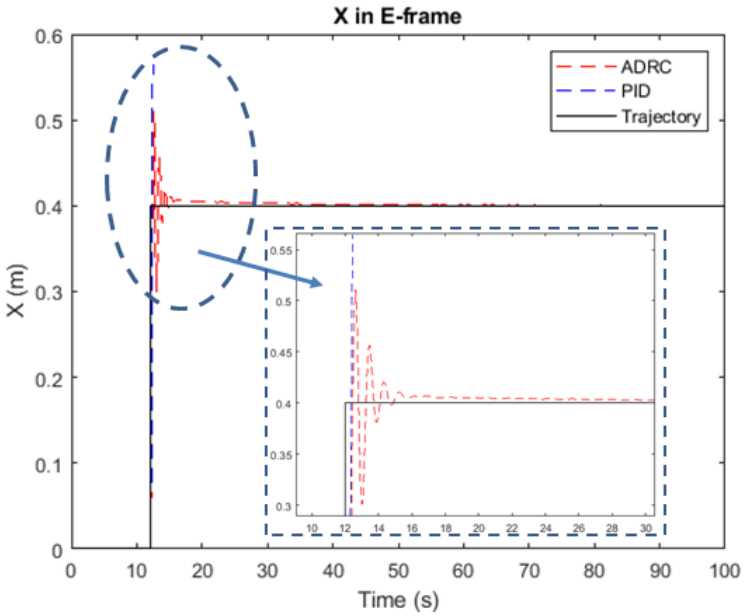

Fig. 4.18: X for 0.4 setpoint

The preceding graphs, reveal the following results: In setpoints 0.1 and 0.3 , the PID does worse on the X coordinate, and better on the Y and Z coordinates than the PD-ADRC, but in general their performance is on par. Beyond the 0.4 setpoint the PID fails, while the PD-ADRC can still balance the system albeit with big amplitude oscillations. The effect of the wind gust and water current on the system, are not visible in the graphs.

4.3 White Noise Test

In this test, the quadrotor will follow a trajectory while being subjected to white noise as discussed before. Two tests will be made with the noise sample time being 0.1 s in the first, and 0.005 s in the second. Wind gusts will be affecting the system from the start, and the water current will start to affect the load when Z equals -0.3, as the quadrotor will lower to an altitude of Z=-0.5 in order to dip the load in the body of water. The first test will have band-limited white noise(of power 0.005 and sample time 0.1 s) added to all three euler angle acceleration equations. The results are:

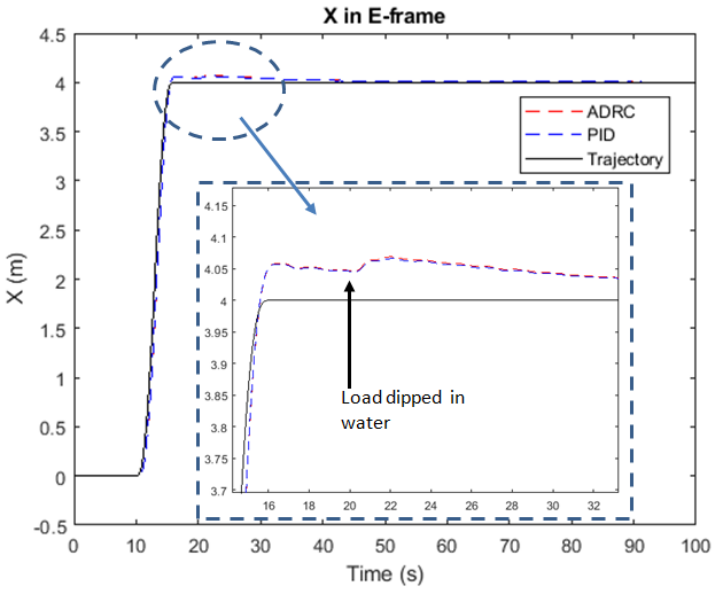

Fig. 4.19: X for 0.1 sample time

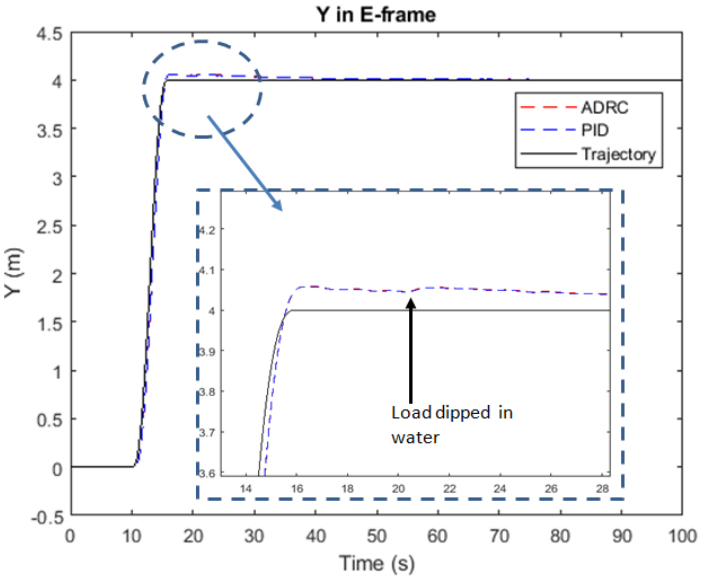

Fig. 4.20: Y for 0.1 sample time

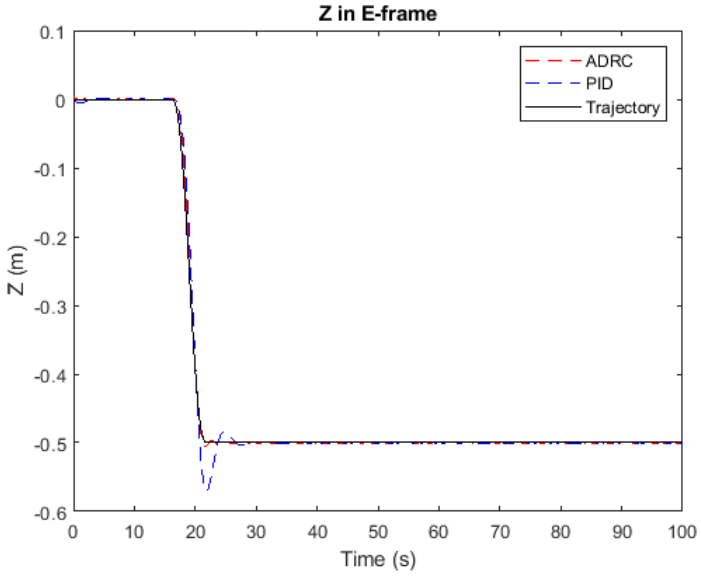

Fig. 4.21: Z for 0.1 sample time

The PID and PD-ADRC have almost the same performance at sample time 0.1s . We also see that the water current is not a fast or strong enough disturbance to differentiate the PD-ADRC from the PID controller.

By lowering the sample time of the noise to 0.005 we get the following graphs:

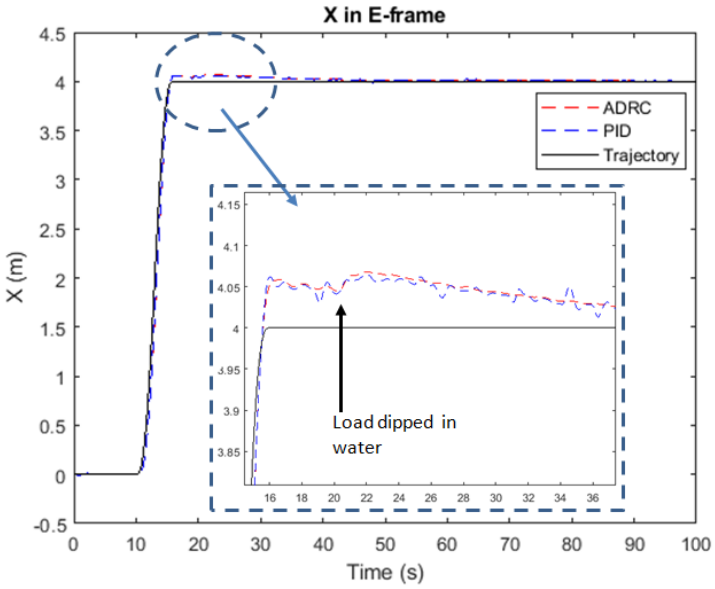

Fig. 4.22: X for 0.005 sample time

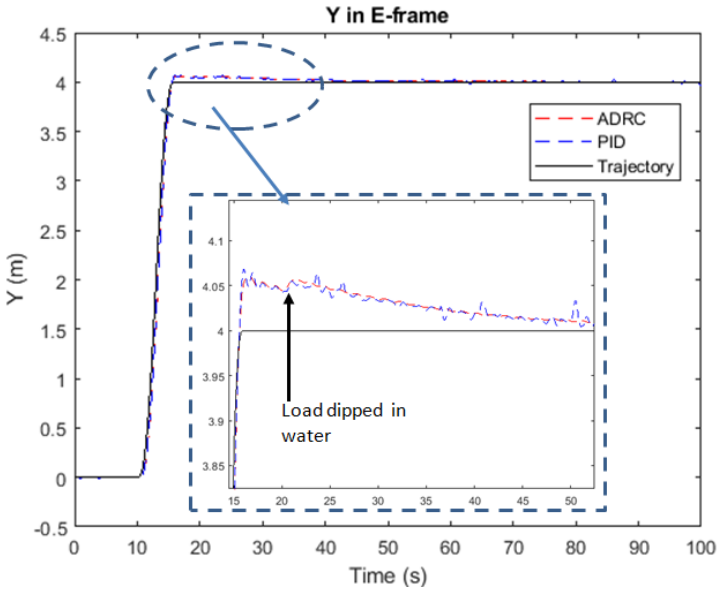

Fig. 4.23: Y for 0.005 sample time

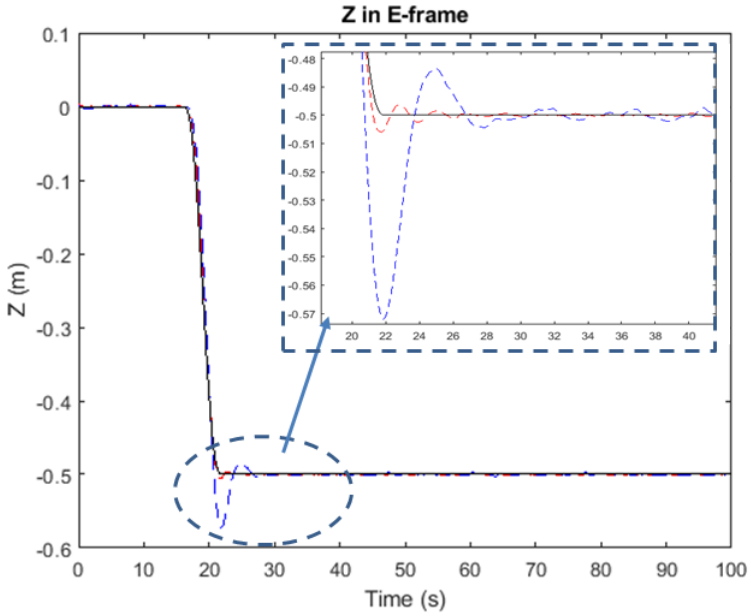

Fig. 4.24: Z for 0.005 sample time

This time the PID's performance is noticeably worse. Small oscillations can be seen in the PID lines, which are not visible in the PD-ADRC ones. Again, as in the setpoint test, we notice that the water current force does not play a deciding role, rather the addition of the white noise brings forth the differences between the two controllers. Lowering even more the sample time or increasing the noise power, further ameliorates the performance of PD-ADRC in comparison with the PID.

Summarising, the previous graphs show that the PD-ADRC scheme is more robust, as it can balance the system at further away setpoints, and has better noise rejection than the normal PID. But the PD-ADRC is as effective at mitigating disturbance in X,Y

as the PIDx and PIDy let it be. In other words, the disturbance rejection efficiency of the PD-ADRC is limited by how fast the PIDx and PIDy controllers are. But making those controllers very fast to stamp out disturbance in X and Y coordinates, can result in a faulty behaviour of the system.

4.4 Concluding Remarks and Improvement Suggestions

What the Results section has shown us so far, is that PD-ADRC is a faster and overall more robust controller than PID when it comes down to following a set angle. These differences though are nullified when the system is asked to follow desired X,Y spatial coordinates, as the speed of convergence of the X,Y coordinates is primarily governed by the PIDx and PIDy and secondarily by the angle controllers. A faster angle controller does not make a big difference when the disturbance is not strong enough, like the water current. To nullify the water currents, stronger PIDx and PIDy controllers are needed.The faster the angle controllers, the faster they'll allow the PIDx and PIDy to be in turn. But when the PIDx , PIDy gains are too high, they tend to destabilise the system and cause unwanted behaviour especially when the setpoint for X and Y is much further away. If the PD-ADRC scheme is to work against tame disturbances like the wind gust and the water current, the controllers of X,Y need to be more sophisticated than simple PIDs. An example of a more sophisticated position controller, based on backstepping sliding-mode control can be found working in tandem with an ADRC angle controller in [16]. [17][18] are further works in a similar direction. All in all, the PD-ADRC with its faster tracking of the desired angles and ability to negate more sudden and powerful disturbances, while retaining the model agnosticism, could prove to be a valid alternative to the standard PID controllers for quadrotors. The cost of two extra tuning parameters and more calculations for the onboard computer, is relatively small when measured against the advantages of the proposed method.

5. APPENDIX

5.1 Euler Angles, Rotation Matrix, and Matrix T_Θ

Euler angles are called the angles of a series of subsequent rotations that bring the earth inertial frame to the attitude of the body-fixed frame. These rotations are as follows:

First a rotation around the Z-axis by a ψ angle. This rotation is expressed by matrix:

$$R_z(\psi) = \begin{bmatrix} \cos(\psi) & -\sin(\psi) & 0 \\ \sin(\psi) & \cos(\psi) & 0 \\ 0 & 0 & 1 \end{bmatrix}$$

Then a rotation around the Y-axis by a θ angle done by matrix:

$$R_y(\theta) = \begin{bmatrix} \cos(\theta) & 0 & \sin(\theta) \\ 0 & 1 & 0 \\ -\sin(\theta) & 0 & \cos(\theta) \end{bmatrix}$$

Finally a rotation around the X-axis by a ϕ angle done by matrix:

$$R_x(\phi) = \begin{bmatrix} 1 & 0 & 0 \\ 0 & \cos(\phi) & -\sin(\phi) \\ 0 & \sin(\phi) & \cos(\phi) \end{bmatrix}$$

Taken together and multiplied in sequence these three give us the following rotation matrix:

$$R_\Theta = R_z(\theta)R_y(\phi)R_x(\theta) =$$
$$= \begin{bmatrix} \cos(\psi)\cos(\theta) & -\sin(\psi)\cos(\phi) + \cos(\psi)\sin(\theta)\sin(\phi) & \sin(\psi)\sin(\phi) + \cos(\psi)\sin(\theta)\cos(\phi) \\ \sin(\psi)\cos(\theta) & \cos(\psi)\cos(\phi) + \sin(\psi)\sin(\theta)\sin(\phi) & -\cos(\psi)\sin(\phi) + \sin(\psi)\sin(\theta)\cos(\phi) \\ -\sin(\theta) & \cos(\theta)\sin(\phi) & \cos(\theta)\cos(\phi) \end{bmatrix}$$

This matrix transforms vectors expressed in the inertial frame to their equivalent in the body frame and vice versa. Say a vector in the inertial frame is defined as $v_I = \begin{bmatrix} v_{I,1} & v_{I,2} & v_{I,3} \end{bmatrix}^T$ and the same vector is defined in the body-frame as: $v_B = \begin{bmatrix} v_{B,1} & v_{B,2} & v_{B,3} \end{bmatrix}^T$. The rotation matrix connects them as follows:

$$v_I = R_\Theta v_B$$

To transform angular velocity from body frame coordinates to Euler angle rates(the derivatives of Euler angles with respect to time) we need a matrix T_θ. Let's say the vehicle's angular velocity in B-frame is given by vector $\omega_B = \begin{bmatrix} p & q & r \end{bmatrix}^T$. We want

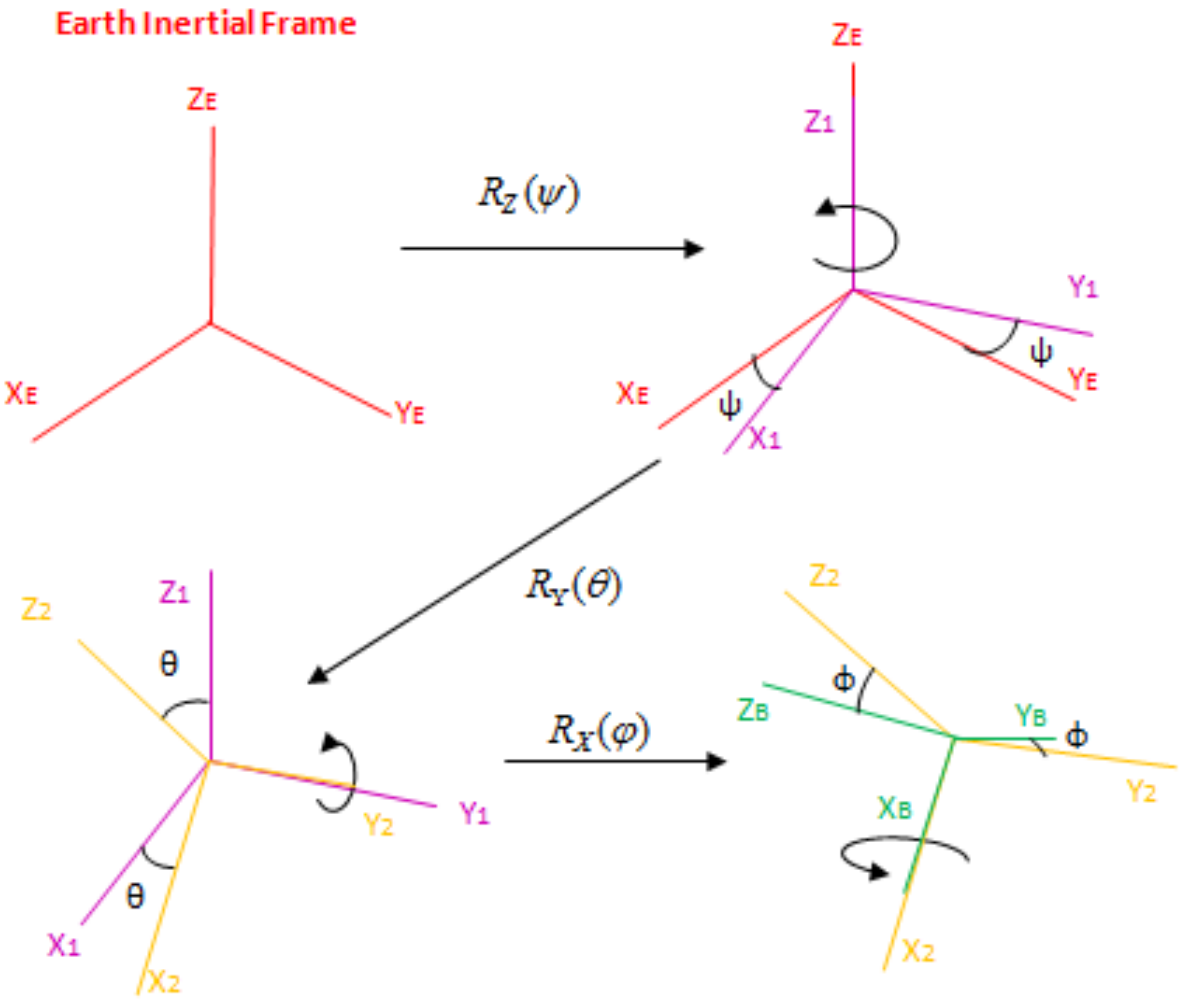

Fig. 5.1: Sequence of Rotations Leading From E-frame(red) to B-frame(green)

to convert this vector to Euler angle rates that is: $\Theta_I = \begin{bmatrix} \dot{\phi} & \dot{\theta} & \dot{\psi} \end{bmatrix}^T$. The following equation gives us this conversion:

$$\begin{bmatrix} p \\ q \\ r \end{bmatrix} = \begin{bmatrix} \dot{\phi} \\ 0 \\ 0 \end{bmatrix} + R(\phi, x)^{-1} \begin{bmatrix} 0 \\ \dot{\theta} \\ 0 \end{bmatrix} + R(\phi, x)^{-1} R(\theta, y)^{-1} \begin{bmatrix} 0 \\ 0 \\ \dot{\psi} \end{bmatrix} = \tag{5.1}$$

$$= \begin{bmatrix} 1 & 0 & -\sin(\theta) \\ 0 & \cos(\phi) & \cos(\theta)\sin(\phi) \\ 0 & -\sin(\phi) & -\cos(\theta)\cos(\phi) \end{bmatrix} \begin{bmatrix} \dot{\phi} \\ \dot{\theta} \\ \dot{\psi} \end{bmatrix} = \mathrm{T}_\Theta{}^{-1} \begin{bmatrix} \dot{\phi} \\ \dot{\theta} \\ \dot{\psi} \end{bmatrix} \tag{5.2}$$

We'll explain how it is derived. Since roll (ϕ) is the final rotation we perform to get the body-frame any additional roll rotation will happen around the X_B axis , naturally. So angle rate $\dot{\phi}$ is expressed directly in the body frame with vector $\begin{bmatrix} \dot{\phi} & 0 & 0 \end{bmatrix}^T$. Any additional pitch rotation ($\dot{\theta}$) will happen in the YELLOW frame of Figure 5.1. So to

convert it to body-frame coordinates we have to premultiply it with $R(\phi, x)^{-1}$. Therefore we get the second term of equation (5.1) : $R(\phi, x)^{-1} \begin{bmatrix} 0 & \dot{\theta} & 0 \end{bmatrix}^T$. Finally, by the same logic any yaw rotation happens in the purple frame of reference in figure 5.1, thus we need to premultiply a yaw rotation given by vector $\begin{bmatrix} 0 & 0 & \dot{\psi} \end{bmatrix}^T$ with $R(\phi, x)^{-1} R(\theta, y)^{-1}$ to express it in the body-fixed reference frame. This gives us the third and final term of equation (5.1).

5.2 Deriving the Inputs U_1, U_2, U_3, U_4

A quadrotor, the particular type of multirotor with four motors, can be approximated quite well by a cross frame with two diametrically opposed motors attached at the end of each bar (Figure 5.2).

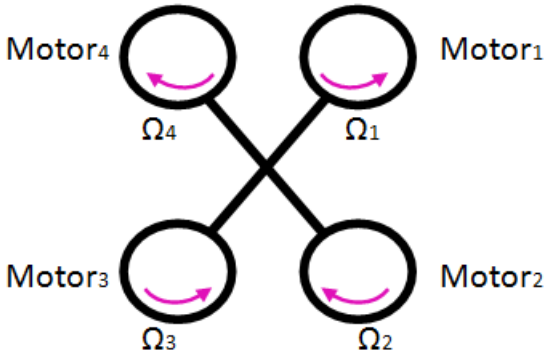

Fig. 5.2: Simplified Quadrotor Structure

Motors 1 and 3 rotate counter-clockwise while motors 2 and 4 rotate clockwise. This difference in rotational direction between the pair of motors guarantees a stable yaw for the vehicle and nullifies the need for a rear propeller like those attached on helicopters. In figure 1 the curved arrows show the direction of rotation of each motor. This configuration permits us to give to the vehicle four independent commands (or inputs in control science terms):

1) Throttle or U_1: This command is the total sum of the thrust force produced by each motor-propeller pair. If the quadrotor's attitude is level with the ground, this command governs the acceleration of the vehicle on Z frame. If the quadrotor is slightly tilted to a side, then this command will also dictate the acceleration on the X and Y axis, as the thrust force is always perpendicular to the quadrotor's frame. Therefore, to move the quadrotor on X and Y axis we tilt it to a side and slightly adjust the throttle so that it uses some upward thrust to hover and some sideways thrust to move around. Considering that the thrust of a propeller equals $b \cdot \Omega^2$ where b is the thrust factor and depends on the propeller, and Ω its rotational speed according to blade element theory (more in [1]), then:

$$U_1 = b({\Omega_1}^2 + {\Omega_2}^2 + {\Omega_3}^2 + {\Omega_4}^2)$$

2) Roll or U_2: This command is achieved by lowering the thrust of motor 2 and raising the thrust of motor 4 or the opposite. This results in the quadrotor tilting around the bar

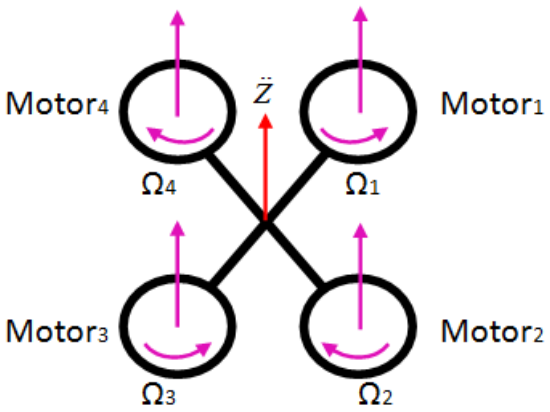

Fig. 5.3: Throttle Showcase

that connect motors 1 and 3. When viewing the movement from the body-fixed frame of the quadrotor, this alters the "roll" angle of the vehicle since the rotation happens around X axis. The total thrust must remain the same so the sum of thrusts of these two motors is kept constant. In other words we lower the speed of one motor as much as we raise the speed of the other. U_2 will be given by:

$$U_2 = lb(-{\Omega_2}^2 + {\Omega_4}^2)$$

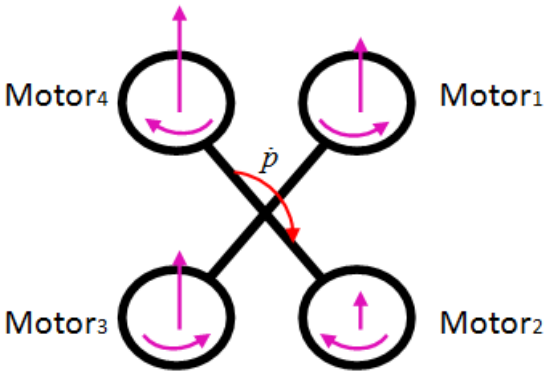

Fig. 5.4: Roll Showcase

3) Pitch or U_3: Similarly, by altering how thrust is partitioned between motors 1 and 3 , it is possible to achieve a tilt around the Y body-frame axis. As is the case with roll, the sum of thrust of the two motors is kept constant so this command leads only to pitch acceleration. U_3 will be given by:

$$U_3 = lb(-{\Omega_1}^2 + {\Omega_3}^2)$$

4) Yaw or U_4: This command lets us rotate the quadrotor around the Z body-frame axis.
Torque around the Z axis is achieved by lowering or raising the thrust of the 1-3 motor pair while simultaneously raising or lowering the thrust of pair 2-4 accordingly so that

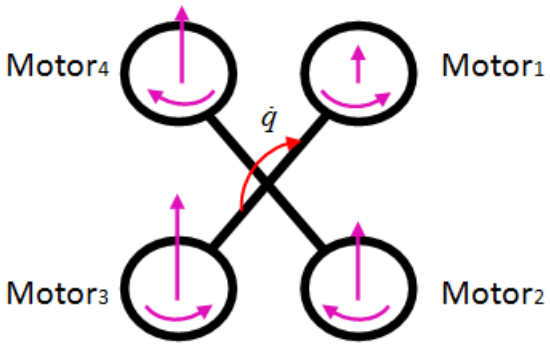

Fig. 5.5: Pitch Showcase

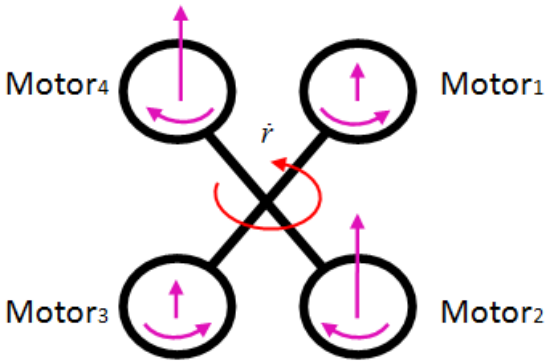

Fig. 5.6: Yaw Showcase

the total thrust remains the same, and no torque is created about X or Y body-frame axis.
This speed imbalance between the motor pairs creates torque about the Z axis.As one pair is pushing the air harder than the other, according to Newton's third law the air's reaction is harder on the faster pair, therefore more force acting on the ends of the bar that connect the two faster motors. The result is torque around the Z axis, its direction opposite to the angular speeds of the fast pair. Finally U_4 equation will be:

$$U_4 = d(-{\Omega_1}^2 + {\Omega_2}^2 - {\Omega_3}^2 + {\Omega_4}^2)$$

where d is the drag factor [1] .

5.3 Gyroscopic effect Torque calculation

As the quadrotor rotates around its center mass, its spinning propellers rotate with it. Because of their spinning they have angular momentums of their own. The four angular momentums of the four propellers need to be rotated with the rest of the quadrotor as they always are perpendicular to the chassis. In order for the rotation of the angular momentum vectors to happen a torque needs to be exercised on the propellers. By Newton's third law the propellers will exercise an opposite torque of equal magnitude on the chassis of the quadrotor, this opposite torque is called the gyroscopic effect and is derived as follows:

Let's say a propeller's angular momentum is symbolised with $H_{pr,E}$ in E-frame and $H_{pr,B}$ in B-frame. Then the rotation matrix connects them as:

$$H_{pr,E} = R_\Theta H_{pr,\mathrm{B}} \tag{5.3}$$

where

$$H_{pr,\mathrm{B}} = \mathbf{\Omega} \cdot J_{TP}$$

with $\mathbf{\Omega}$ being the rotational speed of the propeller in B-frame and J_{TP} its moment of inertia. By derivation with respect to time (5.3) becomes:

$$\frac{d}{dt}H_{pr,E} = \frac{d}{dt}(R_\Theta)H_{pr,B} + R_\Theta\frac{d}{dt}(\mathbf{\Omega})J_{TP} \tag{5.4}$$

By considering that

$$\frac{d}{dt}(\mathbf{\Omega}) = 0$$

and that the time derivative of the angular momentum equals torque:

$$\frac{d}{dt}H_{pr,E} = GyroTorque_E$$

equation (5.4) expands as follows:

$$\begin{aligned}
&GyroTorque_E = S(\omega_E)R_\Theta H_{pr,\mathrm{B}} \Rightarrow \\
&GyroTorque_E = \omega_E \times R_\Theta H_{pr,\mathrm{B}} \Rightarrow \\
&GyroTorque_E = (R_\Theta\omega_B) \times (R_\Theta H_{pr,\mathrm{B}}) \Rightarrow \\
&R_\Theta GyroTorque_B = R_\Theta(\omega_B \times H_{pr,\mathrm{B}}) \Rightarrow \\
&GyroTorque_B = (\omega_B \times \mathbf{\Omega}J_{TP})
\end{aligned}$$

Therefore, we have an expression for the gyroscopic effect of one propeller. To find the combined effect of the four propellers on the quadrotor we sum each torque:

$$\begin{aligned}
&GE_B = -(GyroTorque_{B,1} + GyroTorque_{B,2} + GyroTorque_{B,3} + GyroTorque_{B,4}) \Rightarrow \\
&GE_B = -(\omega_B \times \mathbf{\Omega}_1 J_{TP} + \omega_B \times \mathbf{\Omega}_2 J_{TP} + \omega_B \times \mathbf{\Omega}_3 J_{TP} + \omega_B \times \mathbf{\Omega}_4 J_{TP}) \Rightarrow \\
&GE_B = -J_{TP}\omega_B \times (\mathbf{\Omega}_1 - \mathbf{\Omega}_2 + \mathbf{\Omega}_3 - \mathbf{\Omega}_4)
\end{aligned}$$

By plugging in the following expressions:

$$\omega_B = \begin{bmatrix} p \\ q \\ r \end{bmatrix}$$

$$\mathbf{\Omega}_k = \begin{bmatrix} 0 \\ 0 \\ (-1)^k\Omega_k \end{bmatrix}, k = 1, 2, 3, 4$$

we finally get:

$$GE_B = -J_{TP} \begin{bmatrix} p \\ q \\ r \end{bmatrix} \times \begin{bmatrix} 0 \\ 0 \\ -1 \end{bmatrix} (\Omega_1 - \Omega_2 + \Omega_3 - \Omega_4) \Rightarrow$$

$$\Rightarrow GE_B = J_{TP} \begin{bmatrix} 0 & 0 & 0 & 0 \\ 0 & 0 & 0 & 0 \\ 0 & 0 & 0 & 0 \\ q & -q & q & -q \\ -p & p & -p & p \\ 0 & 0 & 0 & 0 \end{bmatrix} \begin{bmatrix} \Omega_1 \\ \Omega_2 \\ \Omega_3 \\ \Omega_4 \end{bmatrix}$$

5.4 Proof of equation: $M(q)\ddot{q} + k(q, \dot{q}) = Q$

In this part, proof of equation (2.3) will be given for reasons of integrity of this thesis. Suppose we have a system of n generalised coordinates included in vector q:

$$q = \begin{bmatrix} q_1 \\ \vdots \\ q_n \end{bmatrix}$$

And A the matrix

$$\mathrm{A} = \begin{bmatrix} a_{11} & \dots & a_{1n} \\ \vdots & \dots & \vdots \\ a_{k1} & \dots & a_{kn} \end{bmatrix}$$

that connects the time derivatives of these coordinates with the velocity vector as $u = A\dot{q}$. Suppose also that each generalised coordinate has an inertia associated with it , and the inertia matrix D, containing all the inertias is diagonal:

$$D = \begin{bmatrix} M_1 & 0 & \dots & 0 \\ 0 & M_2 & \dots & 0 \\ \vdots & \vdots & \ddots & \vdots \\ 0 & 0 & \dots & M_k \end{bmatrix}$$

We denote that the Lagrangian of the system is equal to the kinetic energy of the body and is given by equation:

$$L = KE = (1/2)u^T Du = (1/2)\dot{q}^T A^T DA\dot{q}$$

By D'Alembert's principle [5], for a rigid body like the quadrotor, we have:

$$\sum_i \left(\vec{F}_i - m_i \dot{\vec{v}}_i\right) \delta\vec{r}_i = 0$$

This sum over all point masses m_i that comprise it must be zero. Virtual work is defined as:

$$\delta W = \sum_i \vec{F}_i \delta\vec{r}_i$$

and, as proven in the Appendix's section 5.5, it holds that:

$$\sum_i m_i \dot{\vec{v}}_i \delta \vec{r}_i = \sum_j \left(\frac{d}{dt} \frac{\partial L}{\partial \dot{q}_j} - \frac{\partial L}{\partial q_j} \right) \delta q_j$$

therefore:

$$\sum_j \left(\frac{d}{dt} \frac{\partial L}{\partial \dot{q}_j} - \frac{\partial L}{\partial q_j} \right) \delta q_j + \delta W = 0$$

or written as a matrix multiplication:

$$\delta q^T \left[\frac{dL}{dq} - \frac{d}{dt} \frac{dL}{d\dot{q}} \right] + \delta W = 0 \tag{5.5}$$

We need to define δW to proceed. Virtual work for a point $\vec{r}_i$ on the quadrotor is: $\delta W_i = \vec{F}_i \delta \vec{r}_i$ where $\vec{F}_i$ is the total vector of forces acting on the point. We can express $\vec{r}_i$ as an addition between vector $\vec{R}_{CM}$, which expresses the position of the quadrotor's center of mass in the inertial frame, and vector $R_\Theta \vec{r}_{i,B}$ which expresses, again in the inertial frame, the vector that connects the center of mass with the point we are analysing(the same vector in B-frame is just $\vec{r}_{i,B}$) :

$$\vec{r}_i = \vec{R}_{CM} + R_\Theta \vec{r}_{i,B}$$

Here R_Θ is the rotation matrix to transform vector $\vec{r}_{i,B}$ from body to inertial frame. Thus, the variance of $\vec{r}_i$ will be:

$$\delta \vec{r}_i = \delta \vec{R}_{CM} + \delta (R_\Theta \vec{r}_{i,B}) \Rightarrow \delta \vec{r}_i = \delta \vec{R}_{CM} + (\delta R_\Theta) \vec{r}_{i,B}$$

with $\delta \vec{r}_{i,B}$ being zero because the point on the quadrotor does not change position in the body frame. For the rotation matrix this equation holds:

$$\delta R_\Theta = S(\delta \vec{\Theta}) R_\Theta$$

where $S(\delta \vec{\Theta})$ is the skew-symmetric matrix of $\delta \vec{\Theta}$, the vector which describes the variance of orientation in the earth frame . Thus using the properties of skew-symmetric matrices we get:

$$\delta \vec{r}_i = \delta \vec{R}_{CM} + (\delta \vec{\Theta}) \times (R_\Theta \vec{r}_{i,B})$$

and finally the virtual work becomes:

$$\delta W_i = \vec{F}_i \delta \vec{R}_{CM} + \vec{F}_i (\delta \vec{\Theta} \times (R_\Theta \vec{r}_{i,B})) = \vec{F}_i \delta \vec{R}_{CM} + \delta \vec{\Theta} (\vec{F}_i \times (R_\Theta \vec{r}_{i,B}))$$

We can then break up $\vec{F}_i$ in two different forces. Forces acting from the outside, and forces acting from the inside between the quadrotor's molecules:

$$\vec{F}_i = \vec{F}_{i,out} + \vec{F}_{i,in}$$

Thus, virtual work is rewritten as the sum over all points N of the quadrotor plus the work of forces acting on the pendulum:

$$\delta W = \sum_{i}^{N} \delta W_i + \delta W_{pen} \Rightarrow$$

$$\Rightarrow \delta W = \sum_{i}^{N} \Big[(\vec{F}_{i,out} + \vec{F}_{i,in}) \delta \vec{R}_{CM} + ((\vec{F}_{i,out} + \vec{F}_{i,in}) \times R_\Theta \vec{r}_{i,B}) \delta \vec{\Theta} \Big] + \vec{F}_{pen,out} \delta \vec{r}_{pen} \tag{5.6}$$

By the properties of a rigid body we have that work attributed to inside forces and inside torques must be equal to zero. That is:

$$\sum_{i}^{N} \vec{F}_{i,in} \delta \vec{R}_{CM} = 0$$
$$\sum_{i}^{N} \Big(\vec{F}_{i,in} \times (R_\Theta \vec{r}_{i,B}) \Big) \delta \vec{\Theta} = 0$$

Therefore we can write the sum of forces on the body as the total force $\vec{F}_{out}$:

$$\sum_{i}^{N} \vec{F}_{i,out} \delta \vec{R}_{CM} = \vec{F}_{out} \delta \vec{R}_{CM}$$

Now, moving on to torque we have:

$$\sum_{i}^{N} \Big[(\vec{F}_{i,out} \times (R_\Theta \vec{r}_{i,B})) \delta \vec{\Theta} \Big] = \vec{T}_{out} \delta \vec{\Theta}$$

We write the inner product of the two vectors in matrix form as:

$$\vec{T}_{out} \delta \vec{\Theta} = {T^T}_{out} \delta \Theta$$

But ${T^T}_{out} = (R_\Theta T_{out,B})^T$ with R_Θ being the rotation matrix. So:

$$(R_\Theta T_{out,B})^T \delta \Theta = {T^T}_{out,B} R_\Theta^T \delta \Theta$$

but $R_\Theta^T = R_\Theta^{-1}$ thus getting both torque and variation of orientation expressed in body-frame coordinates:

$${T^T}_{out,B} R_\Theta^T \delta \Theta = {T^T}_{out,B} R_\Theta^{-1} \delta \Theta = {T^T}_{out,B} \delta \Theta_B = \vec{T}_{out,B} \delta \vec{\Theta}_B$$

Now that everything is in the shape we want, we can write relation (5.6) as:

$$\delta W = \vec{F}_{out} \delta \vec{R}_{CM} + \vec{T}_{out,B} \delta \vec{\Theta}_B + \vec{F}_{pen,out} \delta \vec{r}_{pen}$$

or in matrix form:

$$\delta W = \begin{bmatrix} \delta X & \delta Y & \delta Z \end{bmatrix} \begin{bmatrix} Fx_{out} \\ Fy_{out} \\ Fz_{out} \end{bmatrix} + \begin{bmatrix} \delta angle_{X_B} & \delta angle_{Y_B} & \delta angle_{Z_B} \end{bmatrix} \begin{bmatrix} Tx_{out} \\ Ty_{out} \\ Tz_{out} \end{bmatrix} +$$
$$+ \begin{bmatrix} \delta x_{pen} & \delta y_{pen} & \delta z_{pen} \end{bmatrix} \begin{bmatrix} Fx_{pen,out} \\ Fy_{pen,out} \\ Fz_{pen,out} \end{bmatrix}$$

Note: $\delta angle_{X_B}$ denotes the variation of angle of rotation around axis X_B of the body frame. Accordingly $\delta angle_{Y_B}$ and $\delta angle_{Z_B}$ for variation of angles around axis Y_B and Z_B. We can define vector $\delta\xi$ as

$$\delta\xi = \begin{bmatrix} \delta X \\ \delta Y \\ \delta Z \\ \delta angle_{X_B} \\ \delta angle_{Y_B} \\ \delta angle_{Y_B} \\ \delta x_{pen} \\ \delta y_{pen} \\ \delta z_{pen} \end{bmatrix}$$

Therefore δW can be rewritten:

$$\delta W = \delta\xi^T \begin{bmatrix} Fx_{out} \\ Fy_{out} \\ Fz_{out} \\ Fx_{pen,out} \\ Fy_{pen,out} \\ Fz_{pen,out} \\ Tx_{B,out} \\ Ty_{B,out} \\ Tz_{B,out} \end{bmatrix} = \delta\xi^T \left[f_a + f_g\right]$$

with f_a and f_g being the vectors that we saw earlier.

Now we'll finally connect the work of the generalised forces with the Euler-Lagrange equation (5.5). As we have seen this equation holds:

$$\frac{d\xi}{dt} = u = A\frac{dq}{dt}$$

therefore:

$$\delta\xi = \mathrm{A}\delta q \Rightarrow \delta\xi^T = \delta q^T A^T \Rightarrow \delta\xi^T \left[f_a + f_g\right] = \delta q^T A^T \left[f_a + f_g\right]$$

so finally: $\delta W = \delta\xi^T \left[f_a + f_g\right] = \delta q^T A^T \left[f_a + f_g\right]$ and substituting in relation (5.5) we get

$$\delta q^T \left[\frac{dL}{dq} - \frac{d}{dt}\frac{dL}{d\dot{q}}\right] + \delta q^T A^T \left[f_a + f_g\right] = 0$$

which leads us to the final expression for the Euler-Lagrange equations:

$$\frac{d}{dt}\frac{dL}{d\dot{q}} - \frac{dL}{dq} = A^T \left[f_a + f_g\right] \tag{5.7}$$

Having proven equation (5.7) we move on to prove equations (2.4) and (2.5). We need to prove:

$$M(q)\ddot{q} + k(q,\dot{q}) = \frac{dL}{dq} - \frac{d}{dt}\frac{dL}{d\dot{q}}$$

Since $L = \frac{1}{2}\dot{q}^T A^T D A \dot{q}$ we can write the Lagrangian in the following form utilising sum symbols:

$$\dot{q}^T A^T D A \dot{q} = \sum_{j=1}^{j=k} \left(M_j \left(\sum_{i=1}^{i=n} a_{ji} \dot{q}_i \right)^2 \right)$$

Next we find the derivative of this quantity with respect to vector q:

$$\frac{d}{dq}(\dot{q}^T A^T D A \dot{q}) = \begin{bmatrix} \frac{d}{dq_1} \\ \frac{d}{dq_2} \\ \vdots \\ \frac{d}{dq_n} \end{bmatrix} \sum_{j=1}^{j=k} \left(M_j \left(\sum_{i=1}^{i=n} a_{ji} \dot{q}_i \right)^2 \right) = \begin{bmatrix} \sum_{j=1}^{j=k} M_j \left[\left(\sum_{i=1}^{i=n} \frac{d}{dq_1} a_{ji} \dot{q}_i \right) \left(\sum_{i=1}^{i=n} a_{ji} \dot{q}_i \right) \right] \\ \sum_{j=1}^{j=k} M_j \left[\left(\sum_{i=1}^{i=n} \frac{d}{dq_2} a_{ji} \dot{q}_i \right) \left(\sum_{i=1}^{i=n} a_{ji} \dot{q}_i \right) \right] \\ \vdots \\ \sum_{j=1}^{j=k} M_j \left[\left(\sum_{i=1}^{i=n} \frac{d}{dq_n} a_{ji} \dot{q}_i \right) \left(\sum_{i=1}^{i=n} a_{ji} \dot{q}_i \right) \right] \end{bmatrix}$$

It is easy to see that $DA\dot{q} = \begin{bmatrix} M_1 \sum_{i=1}^{i=n} a_{1i} \dot{q}_i \\ M_2 \sum_{i=1}^{i=n} a_{2i} \dot{q}_i \\ \vdots \\ M_k \sum_{i=1}^{i=n} a_{ki} \dot{q}_i \end{bmatrix}$

The Jacobian of vector $A\dot{q}$ with respect to q is:

$$\nabla_q{}^T (A\dot{q}) = \begin{bmatrix} \sum_{i=1}^{i=n} \frac{d}{dq_1} a_{1i} \dot{q}_i & \sum_{i=1}^{i=n} \frac{d}{dq_2} a_{1i} \dot{q}_i & \dots & \sum_{i=1}^{i=n} \frac{d}{dq_n} a_{1i} \dot{q}_i \\ \sum_{i=1}^{i=n} \frac{d}{dq_1} a_{2i} \dot{q}_i & \sum_{i=1}^{i=n} \frac{d}{dq_2} a_{2i} \dot{q}_i & \dots & \sum_{i=1}^{i=n} \frac{d}{dq_n} a_{2i} \dot{q}_i \\ \vdots & \vdots & \vdots & \vdots \\ \sum_{i=1}^{i=n} \frac{d}{dq_1} a_{ki} \dot{q}_i & \sum_{i=1}^{i=n} \frac{d}{dq_2} a_{ki} \dot{q}_i & \dots & \sum_{i=1}^{i=n} \frac{d}{dq_n} a_{ki} \dot{q}_i \end{bmatrix} = G$$

Now we move on to expand the Euler-Lagrange equation. For the first term $\frac{d}{dt}\frac{dL}{d\dot{q}}$ we have:

$$\frac{d}{dt}\left[\frac{dL}{d\dot{q}}\right] = \frac{d}{dt}\left[A^T D A \dot{q}\right] = A^T D A \ddot{q} + A^T D \dot{A} \dot{q} + \dot{A}^T D A \dot{q}$$

and for the second $\frac{dL}{dq}$:

$$\frac{dL}{dq} = \frac{d}{dq}(\dot{q}^T A^T D A \dot{q}) = \begin{bmatrix} \sum_{j=1}^{j=k} M_j \left[\left(\sum_{i=1}^{i=n} \frac{d}{dq_1} a_{ji}\dot{q}_i \right) \left(\sum_{i=1}^{i=n} a_{ji}\dot{q}_i \right) \right] \\ \sum_{j=1}^{j=k} M_j \left[\left(\sum_{i=1}^{i=n} \frac{d}{dq_2} a_{ji}\dot{q}_i \right) \left(\sum_{i=1}^{i=n} a_{ji}\dot{q}_i \right) \right] \\ \vdots \\ \sum_{j=1}^{j=k} M_j \left[\left(\sum_{i=1}^{i=n} \frac{d}{dq_n} a_{ji}\dot{q}_i \right) \left(\sum_{i=1}^{i=n} a_{ji}\dot{q}_i \right) \right] \end{bmatrix} = G^T D A \dot{q}$$

Putting these two together we get:

$$\frac{d}{dt}\frac{dL}{d\dot{q}} - \frac{dL}{dq} = A^T [f_a + f_g] \Rightarrow A^T D A \ddot{q} + A^T D \dot{A} \dot{q} + (\dot{A} - G)^T D A \dot{q} = A^T [f_a + f_g]$$

Thus we have successfully proven that:

$$M(q)\ddot{q} + k(q, \dot{q}) = Q$$

where

$$\begin{aligned} M &= A^T D A \\ k &= A^T D \dot{A} \dot{q} + (\dot{A} - G)^T D A \dot{q} \\ Q &= A^T (f_a + f_g) \end{aligned}$$

Form $M(q)\ddot{q} + k(q, \dot{q}) = Q$ is really handy because it enables us to have all the dynamics of the system in a compact form expressed by matrices. Easily, we can solve for $\ddot{q}$ as we saw earlier: $\ddot{q} = (A^T D A)^{-1}(Q - A^T D \dot{A} \dot{q} - (\dot{A} - G)^T D A \dot{q})$. This final form enables us to simulate the system much faster as we can calculate numerically each matrix separately and then perform inversions and multiplication of numerical matrices, which is easy on the processor. The alternative would be to have explicit symbolical expressions for each element of $\ddot{q}$, but that would mean someone would have to calculate matrix $(A^T D A)^{-1}$ symbolically, and then multiply it with all these symbolical terms in $(Q - A^T D \dot{A} \dot{q} - (\dot{A} - G)^T D A \dot{q})$. Suffice to say that the expression for each element of $\ddot{q}$ can fill by itself a small handbook! It could be possible to manipulate the matrix with Gauss-Jordan elimination procedure to simplify it considerably, and then find the inverse but this is an intensive exercise in linear algebra and that's outside the scope of this thesis.

5.5 *Proof of equation:* $\sum_i m_i \dot{\vec{v}}_i \delta \vec{r}_i = \sum_j \left(\frac{d}{dt}\frac{\partial L}{\partial \dot{q}_j} - \frac{\partial L}{\partial q_j} \right) \delta q_j$

Proving this relation requires proving first two other equations. We'll show for every vector $\vec{r}$ and vector $\vec{q}$, that these two following relations are in effect:

$$\frac{\partial \vec{r}}{\partial q} = \frac{\partial \dot{\vec{r}}}{\partial \dot{q}} \tag{5.8}$$

$$\frac{d}{dt}\frac{\partial \vec{r}}{\partial q_j} = \frac{\partial \dot{\vec{r}}}{\partial q} \tag{5.9}$$

Relation (5.8) is proven by remembering that from the theory of variances we have:

$$\delta\vec{r} = \sum_j \frac{\partial\vec{r}}{\partial q_j}\delta q_j + \frac{\partial\vec{r}}{\partial t}\delta t$$

By dividing with δt and then differentiating by $\dot{q}_k$ where k denotes one of the components of vector q we get:

$$\frac{\delta\vec{r}}{\delta t} = \vec{v} = \sum_j \frac{\partial\vec{r}}{\partial q_j}\dot{q}_j + \frac{\partial\vec{r}}{\partial t} \Rightarrow \frac{\partial v}{\partial\dot{q}_k} = \frac{\partial\vec{r}}{\partial q_k}$$

For relation (5.9) we notice that:

$$\frac{\partial\vec{v}}{\partial q_k} = \sum_j \frac{\partial^2\vec{r}}{\partial q_k\partial q_j}\dot{q}_j + \frac{\partial^2}{\partial q_k\partial t}\vec{r}$$

and:

$$\frac{d}{dt}\left(\frac{d\vec{r}}{dq_k}\right) = \sum_j \frac{\partial^2\vec{r}}{\partial q_j\partial q_k}\dot{q}_j + \frac{\partial^2}{\partial t\partial q_k}\vec{r}$$

Since the sequence of derivation does not matter we can equate them, thus getting the equation we wanted:

$$\frac{d}{dt}\frac{\partial\vec{r}}{\partial q_j} = \frac{\dot{\partial}\vec{r}}{\partial q}$$

Moving onward to prove relation: $\sum_i m_i\dot{\vec{v}}_i\delta\vec{r}_i = \sum_j \left(\frac{d}{dt}\frac{\partial L}{\partial\dot{q}_j} - \frac{\partial L}{\partial q_j}\right)\delta q_j$, we have:

$$\sum_i m_i\dot{\vec{v}}_i\delta\vec{r}_i = \sum_i m_i\dot{\vec{v}}_i\left(\sum_j \frac{\partial\vec{r}_i}{\partial q_j}\delta q_j\right) =$$
$$= \sum_j\sum_i m_i\dot{\vec{v}}_i\frac{\partial\vec{r}_i}{\partial q_j}\delta q_j = \sum_j \frac{d}{dt}\left(\sum_i m_i\vec{v}_i\frac{\partial\vec{r}_i}{\partial q_j}\delta q_j\right) - \sum_j\sum_i m_i\vec{v}_i\frac{d}{dt}\left(\frac{\partial\vec{r}_i}{\partial q_j}\right)\delta q_j =$$
$$= \sum_j \frac{d}{dt}\left(\sum_i m_i\vec{v}_i\frac{\partial\vec{v}_i}{\partial\dot{q}_j}\delta q_j\right) - \sum_j\sum_i m_i\vec{v}_i\left(\frac{\partial\vec{v}_i}{\partial q_j}\right)\delta q_j = \sum_j\left(\frac{d}{dt}\left(\sum_i m_i\vec{v}_i\frac{\partial\vec{v}_i}{\partial\dot{q}_j}\right) - \sum_i m_i\vec{v}_i\left(\frac{\partial\vec{v}_i}{\partial q_j}\right)\right)\delta q_j =$$
$$= \sum_j\left(\frac{d}{dt}\frac{\partial L}{\partial\dot{q}_j} - \frac{\partial L}{\partial q_j}\right)\delta q_j$$

5.6 Constants

- Motor Dynamics Constants:

  $N = 5.6$ gear box reduction ratio

  $K_M = 6.3 \cdot 10^{-3}$ mechanic motor constant

  $K_E = 6.3 \cdot 10^{-3}$ electric motor constant

  $J_P = 72.8 \cdot 10^{-6}$ rotational moment of inertia around the propeller axis

  $J_M = 1.1 \cdot 10^{-6}$ rotational moment of inertia around the motor axis

  $\eta = 0.9$ gear box efficiency

  $R = 0.6\,\Omega$ motor resistance

- Linearised Motor Dynamics Constants:

  $A_P = -22.7$ linearised propeller's speed coefficient

  $B_P = 514$ linearised constant coefficient

  $C_P = 494$ linearised input voltage coefficient

- Aerodynamic Constants:

  $d = 1.1 \cdot 10^{-6}$ drag factor

  $b = 54.2 \cdot 10^{-6}$ thrust factor

- Quadrotor Characteristics Constants:

  $m = 1\,kg$ mass of quadrotor

  $g = 9.8\ m/s^2$ gravitational acceleration

  $l = 0.24\ m$ length of a quadrotor "arm", from motor to CM.

  $I_{XX} = 8.1 \cdot 10^{-3}\ kg \cdot m^2$ body moment of inertia around the x-axis

  $I_{YY} = 8.101 \cdot 10^{-3}\ kg \cdot m^2$ body moment of inertia around the y-axis

  $I_{ZZ} = 14.2 \cdot 10^{-3}\ kg \cdot m^2$ body moment of inertia around the z-axis

  $J_{TP} = 104 \cdot 10^{-6}\ kg \cdot m^2$ total rotational moment of inertia around the motor axis

  $r_{pen} = 0.05\ m$ distance from quadrotor's CM to attachment point of cable

- Slung-load Constants:

  $m_{pen} = 0.1\ kg$ mass of load

  $L = 0.25\ m$ length of cable.

6. REFERENCES

[1]: Bresciani,T. (2008) . Modelling Identification and Control of a Quadrotor Helicopter. Lund University. Lund. 184 pp.

[2]: Leine,R. Capobianco,G. Bartelt,P. Christen,M. Caviezel,A. (2021). Stability of rigid body motion through an extended intermediate axis theorem: application to rockfall simulation. Multibody System Dynamics. 52. 10.1007/s11044-021-09792-y.

[3]: Cheng,Z. Lei,G.(2020). Towards a theoretical Foundation of PID Control for Uncertain Nonlinear Systems.

[4]: Cicolani,L.S. and Kanning, G. (1992). Equations of Motion of Slung-Load Systems, Including Multilift Systems. NASA. NASA-TP-3280.

[5]: Shapiro,J.A. (2003). Classical Mechanics. Rutgers. 252 pp.

[6]: Stutts,D.S. (2017). Analytical Dynamics: Lagrange's Equation and its Application. University of Science and Technology, Missouri. 23 pp.

[7]: J. Han,(2009),"From PID to Active Disturbance Rejection Control," in IEEE Transactions on Industrial Electronics, vol. 56, no. 3, pp. 900-906

[8]: Qing Zheng,L. Gaol,Q. and Gao,Z. (2007). On stability analysis of active disturbance rejection control for nonlinear time-varying plants with unknown dynamics. 2007 46th IEEE Conference on Decision and Control. 3501-3506 pp.

[9]:Guo, Bao-Zhu and Zhao,Z. (2011). On the convergence of extended state observer for nonlinear systems with uncertainty. Systems and Control Letters. 60. 420-430. 10.1016/j.sysconle.2011.03.008.

[10] Zhao,Z. and Guo,B.(2012). On convergence of nonlinear active disturbance rejection control for MIMO systems. Proceedings of the 31st Chinese Control Conference. pp. 434-441.

[11]: Yang,H. Cheng,L. Xia,Y. and Yuan,Y. (2018). Active Disturbance Rejection Attitude Control for a Dual Closed-Loop Quadrotor Under Gust Wind. in IEEE Transactions on Control Systems Technology. vol. 26, no. 4, pp. 1400-1405

[12]: Chenlu,W. Zengqiang,C. Qinglin,S. and Qing,Z.(2016).Design of PID and ADRC based quadrotor helicopter control system. Chinese Control and Decision Conference (CCDC) pp. 5860-5865

[13]: Huang,Y. Xue,W. .(2014). Active disturbance rejection control: Methodology and theoretical analysis.ISA Transactions.Volume 53, Issue 4. Pages 963-976. ISSN 0019-0578.

[14]: Siciliano, B. Sciavicco, L. Villani, L. Oriolo, G.(2009). Robotics: Modelling, Planning and Control. Springer-Verlag London. 632 pp. ISSN 1439-2232

[15]: Hehn,M. D'Andrea,R.(2011). A flying inverted pendulum. 2011 IEEE International Conference on Robotics and Automation pp. 763-770

[16]: Xu,L.-X. Ma,H.-J. Guo,D. Xie,A.-H. and Song,D.-L. (Dec. 2020). Backstepping Sliding-Mode and Cascade Active Disturbance Rejection Control for a Quadrotor UAV. in IEEE/ASME Transactions on Mechatronics. volume 25. number 6. 2743-2753 pp.

[17]:Besnard L. , Shtessel Y. B., Landrum B. (2012). Quadrotor vehicle control via sliding mode controller driven by sliding mode disturbance observer. Journal of the Franklin Institute. Volume 349. Issue 2. Pages 658-684. ISSN 0016-0032.

[18]: Mahmoud, M. S. Maaruf, M .(2020). Robust Adaptive Multilevel Control of a Quadrotor, in IEEE Access, vol. 8, pp. 167684-167692.